STAMP: Lightweight TEE-Assisted MPC for Efficient Privacy-Preserving Machine Learning

Pengzhi Huang
Cornell University

Thang Hoang
Virginia Tech

Yueying Li
Cornell University

Elaine Shi
Carnegie Mellon University

G. Edward Suh
Meta AI / Cornell University

Abstract

In this paper, we propose STAMP, an end-to-end 3-party MPC protocol for efficient privacy-preserving machine learning inference assisted by a lightweight TEE (LTEE), which will be far easier to secure and deploy than today's large TEEs. STAMP provides three main advantages over the state-of-the-art; (i) STAMP achieves significant performance improvements compared to state-of-the-art MPC protocols, with only a small LTEE that is comparable to a discrete security chip such as the Trusted Platform Module (TPM) or on-chip security subsystems in SoCs similar to the Apple enclave processor. In a semi-honest setting with WAN/GPU, STAMP is $4\times$-$63\times$ faster than Falcon (PoPETs'21) and AriaNN (PoPETs'22) and $3.8\times$-$12\times$ more communication efficient. We achieve even higher performance improvements in a malicious setting. (ii) STAMP guarantees security with abort against malicious adversaries under honest majority assumption. (iii) STAMP is not limited by the size of secure memory in a TEE and can support high-capacity modern neural networks like ResNet18 and Transformer.

1 Introduction

As the world increasingly relies on machine learning for everyday tasks, a large amount of potentially sensitive or private data need to be processed by machine learning algorithms. At the same time, in many cases, cooperation between different entities is also required. For example, machine learning models for medical applications may need to use private datasets distributed in multiple nations as inputs [29]. A cloud-based machine learning services process private data from users with pre-trained weights to provide predictions [1, 16]. The data to be shared in these applications are often private and sensitive and must be protected from the risk of leakage. Government regulations may play an essential role as a policy, but cannot guarantee actual protection. We need technical protection for privacy-preserving machine learning (PPML) for strong confidentiality and privacy guarantees.

Secure multiparty computation (MPC) refers to a protocol that allows multiple participants to jointly evaluate a particular problem while keeping their inputs from being revealed to each other. Ever since Yao's initial studies (later called Garbled Circuit) [73, 74] which gave such a secure protocol in the case of two semi-honest parties, many studies have been conducted to improve the efficiency further, to expand to more than two parties, and to ensure the feasibility against malicious behaviors. Recently, there has been significant interest in using and optimizing MPC for secure machine learning computation [44, 67, 68, 57, 31]. However, the overhead for MPC-based PPML is still significant.

The trusted execution environment (TEE) introduces hardware-based protection by guaranteeing the confidentiality and integrity of data and code inside and provides an opportunity to provide more efficient protection. For example, researchers have proposed to improve MPC by taking advantage of the TEE such as Intel SGX [9]. The tamper-proof feature of SGX can be used in accelerating certain bootstrapping [30, 40] or directly improve overall performance by simplifying the major protocols [8, 2, 30, 12]. However, it is challenging to build a secure environment inside a high-performance processor due to its large trusted computing base (TCB) and complex performance optimizations. For example, multiple attacks have been shown for SGX [65, 64, 17]. TEEs are also proposed for application-specific accelerators or GPUs [22]. However, developing and deploying a TEE for a new piece of hardware requires significant effort and time. The TEE also requires a key infrastructure and trust in its designer and manufacturer, which makes it challenging to have a TEE for each type of hardware. Ideally, TEE protection will be much easier to secure and deploy if the TEE is based on small and simple hardware decoupled from the main computing hardware.

In this paper, we introduce a new PPML framework, named STAMP (Small Tee Assisted MPc), which combines an MPC protocol with a lightweight TEE (LTEE) to reduce MPC overhead while avoiding challenges in a high-performance TEE. For security and ease of deployment, we propose to use a

small TEE comparable to today's trusted platform module (TPM)[1] or on-chip security subsystems such as the Apple enclave processor. Clearly, such lightweight TEEs can only provide relatively low performance. The main question is if a low-performance TEE can still be leveraged to provide meaningful speed-ups for MPC.

The key insight we leverage in STAMP is that non-linear operations, which can be performed very efficiently in plaintext, account for the major part of the overhead in MPC. MPC-based deep learning inference is not particularly expensive in computation but introduces large communication overhead due to multi-round data exchanges, especially when the network latency is high. This overhead leads to a very different cost distribution for MPC compared to plaintext computation. Profiling an inference task of AlexNet [33], which represents a classical deep learning model, shows that 85% of total plaintext execution time comes from linear operations such as convolution and fully-connected layers, while for MPC, this portion drops to only 5% with the remaining 95% coming from non-linear operations. Most of those non-linear operations are simple and cheap in plaintext (e.g., ReLU, MaxPooling, which are generally comparisons) with some exceptions (e.g., Softmax) which has higher complexity. This observation implies that even a lightweight TEE has the potential to significantly speed up MPC-based PPML if we can efficiently offload non-linear operations.

STAMP combines the advantages of MPC and TEE by performing linear operations in MPC for its security and ease of deployment, while leveraging LTEE for non-linear operations. To realize this approach, we introduce new MPC protocols that efficiently offload non-linear operations while minimizing communications among multiple parties and between the LTEE and an untrusted CPU/GPU. Although simple non-linear operations can be performed inside the small LTEE with sufficiently high performance, expensive operations such as Softmax require higher performance. To address these challenges, STAMP securely offloads parts of the expensive exponentiation operations. The following describes the main technical contributions and advantages of STAMP.

Overhead reduction. STAMP achieves significantly lower inference overhead compared to state-of-the-art MPC protocols with either CPU or GPU, under either a WAN or LAN setting. For various networks, the speedup can be $4\times$ to $63\times$, even with a tiny LTEE with a low-bandwidth interconnect. Our analysis shows, as expected, the reduction of external network communication for protocols realizing non-linear functions significantly contributes to the speedup, and the linear operations now become a major part of overhead even in a GPU/WAN setting where computation is fast and communication is slow. We demonstrate that even with trust in a tiny piece of TPM-like hardware, significant speedups can be achieved for privacy-preserving neural network inference.

Malicious security. STAMP provides security guarantees under the honest-majority setting similar to previous schemes [68, 44], assuming that the majority (2 out of the 3 participants) are behaving honestly. If the corrupted party behaves semi-honestly, the protocol ensures that no information is obtained by any party without reconstructing a value. If a party is actively corrupted and behaves maliciously, we guarantee detection of any such behavior and output "abort" while still keeping the confidentiality of the data, with additional overhead compared to the semi-honest setting. We show the security of STAMP using the standard simulation-based paradigm in Appendix B. We implement both semi-honest and malicious protocols in our end-to-end framework, providing an option to choose either lower overhead or higher security guarantees based on the knowledge of the participants.

Evaluation and analysis. We implement STAMP in both CPU-only and GPU-assisted settings, and add the same GPU support to our baseline for a fair comparison. We demonstrate STAMP by supporting the secure inference of various networks including AlexNet [33], VGG16 [59], ResNet18 [21] and Transformer [71], over multiple datasets including MNIST [10], CIFAR-10 [32], ImageNet [56] and Wikitext-2 [42], under both WAN and LAN, and semi-honest and malicious settings. We provide theoretical analysis on the overhead and also perform detailed experimental studies, which show the advantages compared to the state-of-the-art protocols. We therefore show that even a very small TEE reduces the overhead of MPC protocols significantly while supporting various high-capacity networks.

Implementation and results. We implement the semi-honest and malicious protocols of STAMP using C++. The compilation framework and a small number of unchanged pure MPC-based operations (see §3.2 and Appendix A) are based on [68]. The baseline framework was significantly modified to incorporate the new protocols for non-linear operations, support for GPUs, support for new networks and datasets, and a better socket library. The experimental results show that in a WAN / GPU setting, STAMP gains a $4\times$ to $63\times$ or $6\times$ to $59\times$ speed-up in semi-honest or malicious settings compared with the state-of-the-art protocols. We achieve relatively smaller ratios with LAN or/and GPU, but still lead in all tests.

2   Model

In this section, we present our system model, threat model, and security model.

---

[1]TPMs and smartcards have been widely deployed for a while and are much easier to protect compared to a TEE on a high-performance processor. It may be possible to implement lightweight TEE with a firmware extension on today's TPM hardware.

2.1 System Model

In our system, there are three parties who would like to run a common ML model together based on the input of individuals. We assume that the model structure is publicly known. We assume that each party consists of two components: an untrusted machine (CPU/GPU) and an LTEE whose computational power is very limited.

We also assume that each party communicates with each other via a secure authenticated communication channel (e.g., SSL). LTEE in each party communicates with each other through its host via their pairwise secure communication channel for data exchange.

2.2 Threat Model

In our setting, we assume that a party or its server is untrusted except for the LTEE. Specifically, we do not trust any of the server's logic that includes a virtual machine monitor, the operating system and drivers, the software that manages storage, etc. We consider an honest majority, meaning that at most one party (except its LTEE) can be malicious. The other two parties can be semi-honest, in which they may try to learn secrets (e.g., inputs or weights provided by other parties) while still following the protocol faithfully. The malicious adversary can deviate arbitrarily from the honest protocol, and its goal can be breaking the integrity of the evaluation by providing incorrect results without being noticed, or breaking the confidentiality of the data by learning the secrets. We also assume that there is no collusion between any of the parties. We also assume that LTEE cannot be broken by an adversary to obtain any data or alter any code execution. That means there exists a Certificate Authority (CA) to validate the LTEE during the initialization. Figure 1 provides an outline of STAMP, where the three LTEEs act as three trusted third parties with established correlations (secret keys).

2.3 Security model

In our system, the goal is to achieve the confidentiality and integrity of the ML model computation in the presence of a malicious adversary. We capture such confidentiality and integrity through simulation-based security [15, 5, 6] in the following definition.

Definition 1 (Simulation-based security: privacy and verifiability). A protocol $\pi_{\mathcal{F}}$ is said to securely realize the ideal functionality $\mathcal{F}$ if for any probabilistic polynomial time (PPT) real-world adversary $\mathcal{A}$, there exists an ideal-world adversary $\mathcal{S}$ such that for any PPT environment $\mathcal{Z}$, there exists a negligible function negl such that

$$|\Pr[\text{Real}_{\Pi_{\mathcal{F}},\mathcal{A},\mathcal{Z}(\lambda)} = 1] - \Pr[\text{Ideal}_{\mathcal{F},\mathcal{S},\mathcal{Z}(\lambda)} = 1]| \leq \text{negl}(\lambda)$$
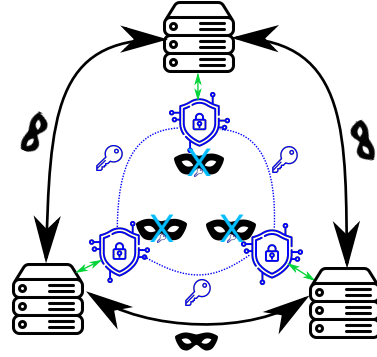

Figure 1: Diagram of participants and their communication channels. The black local machines owned by parties are untrusted and the the blue LTEEs are trusted, with green local bus, black inter-party channel to communicate. Blue keys are shared among LTEEs.

3 Background

In this section, we discuss the background materials for our method. We first describe our notation, and then provide some prelims of MPC and TEE.

3.1 Notation

We define L to be the finite field size, and $\mathbb{Z}_L$ to be the finite field we are generally considering in this work. fp is the fixpoint precision. We use the bold font $\mathbf{a}$ or $\mathbf{A}$ to represent a vector or a matrix. We use a_i or $A_{i,j}$ to represent the ith element of the vector $\mathbf{a}$ or the element of the matrix $\mathbf{A}$ in the ith row and the jth column. This is different from the bold $\mathbf{A}_i$, which still represents a matrix. Throughout the paper, if not specifically mentioned, all operations are carried out within the finite field $\mathbb{Z}_L$. When needed, we use $(a+b)_L$ to represent the modulo L operation for the output of the integer operations in brackets. We add a bar to a variable or operation, as $\bar{a}, \overline{\exp(a)}$, to represent that a number or an output is a real number. The right-shift operation is indicated as $\gg$ (e.g. $a \gg b = a/2^b$). We will often use two signed integers m, q to represent a positive real number $\bar{a}$ as $\bar{a} = 2^q \cdot (m \gg 52)$ where m represents the mantissa part of 52 bits with $m \gg 52 \in [0, 1)$, and q_L is the exponent part. This is actually the format in which floating point numbers are represented following the IEEE Standard for Binary Floating-Point Arithmetic (IEEE 754-1985) [28], but without sign on the mantissa part. We use $\lfloor \bar{a} \rceil$ to round a real number $\bar{a}$ down to an integer.

3.2 Multiparty Computation

Notation. The sharing scheme we consider in this work is 2-out-of-3 replicated secret sharing scheme (RSS) modulo L.

Let P_1, P_2, P_3 be the three parties participating in the evaluation. For convenience in notation, we use P_{i-1}, P_{i+1} to refer to the previous and next party of one party (e.g., the previous and the next party of P_1 are P_3 and P_2). The RSS of an integer secret $x \in \mathbb{Z}_L$ is denoted as $[\![x]\!]^L = ([\![x]\!]_1^L, [\![x]\!]_2^L, [\![x]\!]_3^L)$, where L is the size of the finite field to which the shares belong and $x = [\![x]\!]_1^L + [\![x]\!]_2^L + [\![x]\!]_3^L$. When we say that a secret x is shared as $[\![x]\!]^L$, it means that party P_i is holding $([\![x]\!]_i^L, [\![x]\!]_{i+1}^L)$ for $i = 1, 2, 3$, so any two of the three parties can recover the plaintext x with their shares combined. To generate the integer representation x based on the real value $\bar{x}$, we use two's complement fixed-point encoding with fp bits of precision. For a positive $\bar{x}$ we have $x = \lfloor \bar{x} \cdot 2^{\mathsf{fp}} \rceil$, while for a negative $\bar{x}$, $x = \lfloor \bar{x} \cdot 2^{\mathsf{fp}} \rceil + L$, assuming that x is within the bound $[-L/2^{\mathsf{fp}}, L/2^{\mathsf{fp}})$. We focus on the cases of $\mathsf{fp} = 13$, $L = 2^l$ and $l = 32$ and in this work (which supports inputs from -262144 to $262144 - 2^{-13}$).

We introduce how multiplications in a can be performed under 2-out-of-3 RSS. These operations are based on the protocols defined in [44, 67, 68] and are mostly linear operations.

Multiplications. $[\![x \cdot y]\!]^L \leftarrow \Pi_{\mathsf{Mul}}([\![x]\!]^L, [\![y]\!]^L)$: To get $[\![z]\!]^L = [\![x \cdot y]\!]^L$, P_i would first compute $\hat{z}_i = x_i y_i + x_{i+1} y_i + x_i y_{i+1}$, then $(\hat{z}_1, \hat{z}_2, \hat{z}_3)$ is already a valid 3-out-of-3 secret sharing of xy since $z_1 + z_2 + z_3 = xy$. A reshare is needed to maintain the consistency of the 2-out-of-3 sharing scheme. To avoid any possible leakage of information, P_i uses the 3-out-of-3 randomness $\{\alpha_i\}$ to mask $\hat{z}_i$ as $z_i = \hat{z}_i + \alpha_i$, then share it with P_{i-1}. Therefore, the parties obtain the necessary shares and $[\![z]\!]^L = [\![xy]\!]^L = (z_1, z_2, z_3)$ is built.

Matrix Multiplications. $([\![\mathbf{A}]\!]^L \times [\![\mathbf{B}]\!]^L) \leftarrow \Pi_{\mathsf{MatMul}}([\![\mathbf{A}]\!]^L, [\![\mathbf{B}]\!]^L)$: To perform matrix multiplication $[\![\mathbf{C}_{a \times c}]\!]^L = [\![\mathbf{A}_{a \times b}]\!]^L \times [\![\mathbf{B}_{b \times c}]\!]^L$ in the RSS scheme, a similar protocol can be used as in Π_{Mul}. While simply applying the same protocol for each multiplication leads to $O(abc)$ shares to be sent, parties can instead perform matrix multiplication locally (i.e., $[\![\hat{\mathbf{C}}]\!]_i^L = [\![\mathbf{A}]\!]_i^L [\![\mathbf{B}]\!]_i^L + [\![\mathbf{A}]\!]_i^L [\![\mathbf{B}]\!]_{i+1}^L + [\![\mathbf{A}]\!]_{i+1}^L [\![\mathbf{B}]\!]_i^L$) and then share the results at once. This strategy yields only $O(ac)$ transmission overhead, saving a factor b of the number of shares to be sent. As stated in [67], convolutions can be expanded into overall larger matrix multiplications.

The above protocols dealing with multiplications work well for integer representations, but will cause errors with fixed-point representations. A truncation protocol (right-shift the results by fp bits) must follow the multiplication to correct the fixed-point precision. [44] provides more details on the 3-party truncation protocol.

We refer the reader to [44, 14] for details of the malicious variant of Π_{MatMul}, and to Appendix A for other basic operations.

3.3 Trusted Execution Environment

A TEE protects the integrity and confidentiality of the code and data inside, even when low-level software and/or the envi-
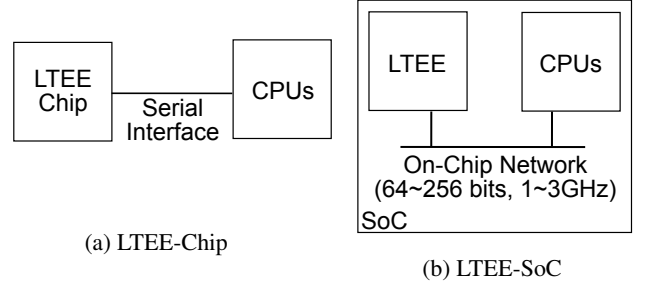

(a) LTEE-Chip

(b) LTEE-SoC

Figure 2: Two types of LTEEs that STAMP considers.

ronment cannot be trusted. The TEE can be implemented on a shared high-performance processor such as Intel SGX [64] or on separate hardware such as TPMs. Existing work on secure machine learning computation mostly utilizes SGX as a high-performance TEE. In this work, we consider a lightweight TEE (LTEE) with capability and complexity similar to a TPM or on-chip security subsystems in modern SoCs: a dedicated low-performance security processor that can support remote attestation to validate its identity while exchange shared keys (§4.1). .

While high-performance TEEs such as Intel SGX can directly run compute-intensive workloads such as machine learning, it is much more difficult to provide high-security assurance or develop/deploy the high-performance TEEs compared to small dedicated security chips or SoC modules. A high-performance CPU contains millions of lines of code (LoCs) [35], takes hundreds of mm^2 in the silicon area, and is shared by many software components. Unfortunately, the large TCB and high complexity often lead to more vulnerabilities, as illustrated by many attacks found for high-performance TEEs, including page-fault-driven attacks [72, 58], segmentation-based attacks [19, 37], CPU cache-based attacks [17, 4], and enclave software attacks [36, 69].

On the other hand, dedicated security processors have a long history of being used successfully in many high-security use cases. For example, smart cards [52] are widely used in financial transactions. Discrete security chips such as TPM [49], Google Titan [24], and Apple T1 provide hardware root-of-trust on many platforms. Modern System-on-Chip (SoC) designs also typically include a dedicated security processor with crypto engines for secure booting and other high-security operations: Synopsys tRoot Hardware Secure Modules [61], Rambus RT-630 Programmable Root of Trust [26], Apple Secure Enclave [23], and Qualcomm Secure Processing Unit [25]. These dedicated security processors usually require less than $1mm^2$. Even though their performance is limited, the small dedicated security processors are far easier to protect and also easier to deploy because they can be integrated as a separate chip or a block on an SoC.

In this work, we consider two types of LTEE designs as shown in Figure 2: 1) a discrete security chip similar to a

TPM (LTEE-chip) and 2) a security subsystem module on an SoC (LTEE-SoC). LTEE-chip typically runs at a low clock frequency (tens of MHz) and connects to a CPU through a low-bandwidth serial interface. LTEE-SoC can run at a much higher SoC clock frequency (1-3GHz) and connects to other processing engines (CPUs, GPUs, NPUs, etc.) on the same SoC through high-bandwidth on-chip networks. Our study suggests that even the discrete LTEE-chip can significantly improve the performance of MPC-based PPML.

Notation. In this work, each party P_i is equipped with a LTEE H_i, and H_i has a built-in PRF unit F for pseudo-random number generation (an AES engine would be enough). We assume that even malicious participants cannot break the integrity and confidentiality guarantee that it provides. Details of the protocols executed in H_i will be introduced in §4, and a further detailed discussion of the hardware can be found in §5.

4 The STAMP Protocol

This section introduces the details of the STAMP protocols in a semi-honest setting and the additional steps needed in a malicious setting. We first describe on the basic ReLU protocol, the optimized ReLU protocol, and how they can be expanded to other common non-linear functions. Then, we finally present the protocol for Softmax.

4.1 Initialization phase

The initialization phase is a part of the offline phase (which needs no input data or model weights) of the protocol where the LTEEs will have shared keys and initial values established in them if their identities are proven. Although Π_{Init} plays an important role in our scheme, it is not where our main contribution lies, since mature remote attestation protocols already exist [3]. A proper remote attestation protocol is commonly supported in secure hardware such as a TPM [49], and validates the LTEE's identity and its state. This process can involve the acquisition of the certificate of a LTEE from a trusted CA/Verifiers, which is usually the manufacturer of the TEE. H_i after being verified, can perform pairwise Diffie-Hellman key exchanges with a signature to obtain the shared key $k_{i-1,i}$ with H_{i-1}, $k_{i,i+1}$ with H_{i+1}, and then also $k_{i+1,i-1}$ through sharing masks. A simplified description of Π_{Init} is shown in Protocol 1.

The communication out of H_i has to go through P_i, which provides a corrupted party with a natural way to observe or even alter the communication among the LTEEs. For semi-honest adversaries, the Diffie–Hellman key exchange protocol already prevents them from obtaining the key with bounded computational resources. If the corrupted party behaves maliciously, Π_{Init} does not have to take extra steps to detect such actions. If a malicious P_i modifies the remote attestation, a CA will not provide a certificate and P_i cannot create a certificate

on its own, causing an abort. If P_i changes the initial parameters or alters the transmission during key exchange, there will be no correct initialization established, and the protocol will abort later when data inconsistency is detected.

Protocol 1 Π_{Init} Initialization

Input. Security parameter λ.
Result. Output $(\mathsf{Success}, L)$ if the remote attestation succeeds and aborts if failed. After the initialization, LTEEs (H_i) obtain shared keys and initial parameters.
  1. Parties first agree to a L for the finite field $\mathbb{Z}_L$, size $l = \log L$ bits, prime p, and their order to define the previous and next party.
  2. P_is perform remote attestation on each H_i to obtain a certificate from the CA and publicly share them to validate H_i. Abort if validation fails.
  3. H_i performs Diffie–Hellman key exchange with signature through the secure channel between P_is to obtain $O(\lambda)$-bit PRF keys $k_{i,i+1}, k_{i-1,i}$, then use $F_{k_{i,i+1}}$ to mask one key $k'_{i-1,i} \equiv k_{i-1,i} + F_{k_{i,i+1}}(0) \mod p$ and send $k'_{i-1,i}$ to H_{i+1} through P_i. H_i would receive $k'_{i+1,i-1}$ from H_{i-1} and can recover $k_{i,i+1} = k'_{i,i+1} - F_{k_{i-1,i}}(0)$.

The shared keys and the PRF in the LTEEs can support the random number generation and are kept only known to the LTEE, unlike the correlated randomness introduced in Appendix A. With the shared keys in §4.1 and a built-in PRF F, we can now construct $\Pi_{\mathsf{LTEE.GenMask}}$ and $\Pi_{\mathsf{LTEE.GenMaskShare}}$ in the LTEE as Protocol 2 and Protocol 3. They are very similar with only a minor difference that $\Pi_{\mathsf{LTEE.GenMaskShare}}$ always generates shares of $\mathbf{0}$. Four counters $\{\mathsf{ctr}_1^i, \mathsf{ctr}_2^i, \mathsf{ctr}_3^i, \mathsf{ctr}_s^i\}$ are used in each H_i to maintain consistency among H_is in a semi-honest setting, and additional four $\{\hat{\mathsf{ctr}}_1^i, \hat{\mathsf{ctr}}_2^i, \hat{\mathsf{ctr}}_3^i, \hat{\mathsf{ctr}}_s^i\}$ are needed in a malicious setting for reduplicate execution for the detection of inconsistency. Notice that Protocol 2 and Protocol 3 give the outputs to H_i, not P_i, and H_i may be set to give partial outputs in some protocols.

Protocol 2 $\mathbf{m} \leftarrow \Pi_{\mathsf{LTEE.GenMask}}(n, L, j; i, \mathsf{ctr}_j^i, k_{j,j+1})$

Input. The number of masks to be generated n, the index j for which counter, and which key to choose. The size of the finite field L, the counter ctr_j^i and the key $k_{j,j+1}$ are stored in the LTEE.
Output. pseudo-random masks $\mathbf{m} \in \mathbf{Z}_L$ and updated counter ctr_j^i.
$\mathbf{m} = (F_{k_{j,j+1}}(\mathsf{ctr}_j^i), F_{k_{j,j+1}}(\mathsf{ctr}_j^i + 1), ..., F_{k_{j,j+1}}(\mathsf{ctr}_j^i + n - 1))$.
Update $\mathsf{ctr}_j^i \leftarrow \mathsf{ctr}_j^i + n$.

4.2 ReLU

Non-linear layers used in a machine learning model are computationally light under plaintext. Π_{ReLU}, for example, takes only one comparison and multiplexing. However, its complexity gets amplified significantly under the RSS scheme with

5

Protocol 3 $(\llbracket \mathbf{m}_j \rrbracket_i^L, \llbracket \mathbf{m}_j \rrbracket_{i+1}^L) \leftarrow \Pi_{\mathsf{LTEE.GenMaskShare}}(n, L;$
$i, \mathsf{ctr}_s^i, k_{i,i+1}, k_{i+1,i-1}, k_{i-1,i})$

Input. The number of masks to be generated n. The size of the finite field L and the counter and keys are stored in the LTEE.

Output. pseudorandom masks $\llbracket \mathbf{m} \rrbracket_i^L, \llbracket \mathbf{m} \rrbracket_{i+1}^L \in \mathbb{Z}_L$

$\llbracket m_j \rrbracket_i^L = F_{k_{i,i+1}}(\mathsf{ctr}_s^i + k) - F_{k_{i+1,i-1}}(\mathsf{ctr}_s^i + k)$ for $k = 0, ..., n-1$

$\llbracket m_j \rrbracket_{i+1}^L = F_{Ki+1,i-1}(\mathsf{ctr}_s^i + k) - F_{Ki-1,i}(\mathsf{ctr}_s^i + k)$ for $k = 0, ..., n-1$

Update $\mathsf{ctr}_s^i \leftarrow \mathsf{ctr}_s^i + n$.

---

more local computation steps and significant communication overhead, both in communication rounds and the amount of transmitted data (we will list and compare the theoretical complexities in Appendix D).

Now, aided by the LTEE held by each party and the common randomness established in §4.1, we can significantly reduce the overhead by "offloading" the non-linear operations to the LTEE. Although the LTEE is far inferior in computation power compared to the untrusted machine, it can still remove much of the communication overhead in a pure MPC protocol.

In this section, we introduce Π_{ReLU}, the protocol to offload ReLU operations under MPC to trusted hardware. The steps we take are as follows: First, P_i invokes $\Pi_{\mathsf{LTEE.GenMask}}$ to get the pseudo-random masks, and sends $\llbracket x \rrbracket_i$ to P_{i+1} after adding them with the masks; Second, P_{i+1} adds the received value with the two shares it holds, then sends the results to the LTEE; Third, H_{i+1} recovers the plaintext value by invoking $\Pi_{\mathsf{LTEE.GenMask}}$ using the same key and the counter with the same recorded number, and computes ReLU in plaintext, re-masks the result with $\Pi_{\mathsf{LTEE.GenMaskShare}}$, and sends them back to P_{i+1}. The other two parties will also generate their common share in the meantime; Fourth, P_{i+1} re-shares the received values to complete the construction of the RSS of the outputs.

Π_{ReLU} is given in Protocol 4 for the semi-honest setting in black. The extra steps marked in blue are only executed when malicious security is needed, and we use this notation in other protocols as well. The malicious version generally adds replicate parallel operations, similar to executing the semi-honest protocol twice. It also requires replicate sharing of the same values to validate the integrity. Parties compare the copies of intermediate results and final outputs from different sources to achieve malicious security with abort.

After the protocol, $\{\mathsf{ctr}_{1,2}^i, \mathsf{ctr}_{2,3}^i, \mathsf{ctr}_{3,1}^i, \mathsf{ctr}_s^i\}$ for $i = 1, 2, 3$ all increase by n, and $\{\hat{\mathsf{ctr}}_{1,2}^i, \hat{\mathsf{ctr}}_{2,3}^i, \hat{\mathsf{ctr}}_{3,1}^i, \hat{\mathsf{ctr}}_s^i\}$ for $i = 1, 2, 3$ all increase by n too in a malicious setting. The synchronization of the counters together with shared keys guarantees the correlated randomness among the LTEEs.

One may notice that the workload is not balanced among the three parties if we fix i. In the protocol, the party index i can be any of $\{1, 2, 3\}$, which means that the three parties can start the protocol simultaneously with a disjoint dataset.

Therefore, when provided with a batch B of inputs for evaluation, each party can work on the $B/3$ data and start the corresponding protocol simultaneously, balancing resource usage and reducing overall latency.

4.3 Further Optimization of ReLU

As introduced in §3.2, in a fixed-point setting, truncation is required after each multiplication to keep the consistency of the precision. The classic MPC protocol [44] requires pregeneration and a round of communication. We also observe that for classical networks [33, 71, 59, 21], the layers containing matrix multiplications such as convolution (Conv) and fully-connected (FC) layers are often applying ReLU to the results at the end. If we apply Protocol 4 directly after the completion of multiplications, the communication overhead will be the multiplication / truncation overhead and the Protocol 4 overhead summed, which is not optimal. Since truncation itself is also a simple non-linear function in plaintext (which is just right-shift), we can exploit this common structure in deep learning models to further reduce the overhead. The way is to merge the communication during the last step of multiplication - the truncation, with the following non-linear operations, which can be simply computed in plaintext inside the trusted LTEE.

The protocol $\Pi_{\mathsf{MatMulReLU}}$ showing how ReLU can be combined with truncation after matrix multiplication is given in Protocol 5. Extra communication has to be done compared to Protocol 4, because the parties hold 3-out-of-3 sharing instead of 2-out-of-3 after local steps of multiplication, as described in §3.2. $\Pi_{\mathsf{MatMulReLU}}$ reduces the total communication rounds of matrix multiplication and ReLU combined to 2 from at least 3, and also saves the total amount of data to be transmitted by merging the step 2) of Protocol 4 with the communication needed during truncation. It is also worth mentioning that as discussed in §4.2, the task of a batch containing multiple inputs can be evenly split among the three parties to balance resource usage. For the malicious setting, we use $\Pi_{\mathsf{mal\text{-}arith\text{-}mult}}$ of [44] to ensure correct 2-out-of-3 shares after local multiplication, then make the replicate execution as we did in Protocol 4.

4.4 Extensions to Other Operations

The protocols mentioned in §4.2 can be extended to common non-linear operations needed in deep learning networks, including $\Pi_{\mathsf{MaxPooling}}, \Pi_{\mathsf{BatchNorm}}, \Pi_{\mathsf{LayerNorm}}$. $\Pi_{\mathsf{MaxPooling}}$ only needs comparisons and multiplexing. $\Pi_{\mathsf{BatchNorm}}$ and $\Pi_{\mathsf{LayerNorm}}$ need about two multiplications for each element on average. Their low complexity allows them to be offloaded to the LTEE in a similar way as Π_{ReLU}. Minor changes are needed in step 4) of Π_{ReLU}. $\Pi_{\mathsf{MatMulReLU}}$ can be extended to others in a similar way, changing step 5) of $\Pi_{\mathsf{MatMulReLU}}$ for other plaintext operations to be performed in the LTEE.

Protocol 4 $[\![\mathsf{ReLU}(\mathbf{x})]\!]^L \leftarrow \Pi_{\mathsf{ReLU}}([\![\mathbf{x}]\!]^L)$ Do ReLU on shares of vector $\mathbf{x}$

Input. Each $\{P_i\}$ owns $[\![\mathbf{x}]\!]^L$.
Output. Each $\{P_i\}$ gets $[\![\mathbf{z}]\!]^L = [\![\mathsf{ReLU}(\mathbf{x})]\!]^L$.

1. P_i calls H_i to execute $\Pi_{\mathsf{LTEE.GenMask}}(n,L,i)$ to obtain the masks $\mathbf{m}_i \in \mathbf{Z}_L^n$ then compute $\mathbf{x}'_i = [\![\mathbf{x}]\!]_i^L + \mathbf{m}_i$.
   Malicious: P_{i-1} generates $\mathbf{m}_i = \Pi_{\mathsf{LTEE.GenMask}}(n,L,i)$ and $\mathbf{x}'_i = [\![\mathbf{x}]\!]_i^L + \mathbf{m}_i$, and P_{i-1}, P_{i+1} also generates $\mathbf{m}_{i+1,i-1} = \Pi_{\mathsf{LTEE.GenMask}}(n,L,i)$, $\mathbf{x}'_{i-1} = [\![\mathbf{x}]\!]_{i-1}^L + \mathbf{m}_{i+1,i-1}$.

2. P_i send $\mathbf{x}'_i$ to P_{i+1}.
   Malicious: P_{i-1} send $\mathbf{x}'_i$ to P_{i+1}, P_{i-1}, P_{i+1} send $\mathbf{x}'_{i-1}$ to P_i

3. P_{i+1}, after receiving $\mathbf{x}'_i$ add it to $[\![\mathbf{x}]\!]_{i+1}^L$, $[\![\mathbf{x}]\!]_{i-1}^L$ and pass it to H_{i+1}.
   Malicious: P_i, P_{i+1} check the two copies received and abort if any inconsistency is found. P_i execute as above with index $i-1$ replacing index i.

4. **LTEE Only** : H_{i+1} recovers the plaintext $\mathbf{x} = (\mathbf{x}'_i + [\![\mathbf{x}]\!]_{i+1}^L + [\![\mathbf{x}]\!]_{i+2}^L) - \mathbf{m}_i$ where $\mathbf{m}_i$ is generated with $\Pi_{\mathsf{LTEE.GenMask}}(n,L,i)$. Set $\mathbf{b} = (\mathbf{x} > \mathbf{0})$. Then H_{i+1} invokes $\Pi_{\mathsf{LTEE.GenMaskShare}}(n,L)$ to get $[\![\mathbf{z}^*]\!]_i^L, [\![\mathbf{z}^*]\!]_{i+1}^L \in \mathbb{Z}_L^n$, and compute: $([\![z_j]\!]_i^L, [\![z_j]\!]_{i+1}^L) = ((b_j?x_j:0) + [\![z_j^*]\!]_i^L, [\![z_j^*]\!]_{i+1}^L)$. Return their values to P_{i+1}.
   H_i and H_{i-1} invokes $\Pi_{\mathsf{LTEE.GenMaskShare}}(n,L)$ to get $[\![\mathbf{z}]\!]_{i-1}^L \in \mathbb{Z}_L^n$, and invokes $\Pi_{\mathsf{LTEE.GenMaskShare}}(n,2)$ to get $[\![\mathbf{b}]\!]_{i-1}^L \in \mathbb{Z}_2^n$. Return them respectively to P_i and P_{i-1}.
   Malicious: H_i perform the same step as above with index $i-1$ replacing index i, replacing $\Pi_{\mathsf{LTEE.GenMaskShare}}$ with $\Pi'_{\mathsf{LTEE.GenMaskShare}}$, while also masking the results with the masks of index i (i.e., $([\![z_j]\!]_{i-1}^L, [\![z_j]\!]_i^L) = ([\![z_j^*]\!]_{i-1}^L, (b_j?x_j:0) + [\![z_j^*]\!]_i^L)$). H_{i-1} and H_{i+1} generate the remaining share for P_{i-1} and P_{i+1} respectively.

5. P_{i+1} send $[\![\mathbf{z}]\!]_i^L$ to P_i, send $[\![\mathbf{z}]\!]_{i+1}^L$ to P_{i-1}. Now $[\![\mathbf{z}]\!]^L$ and $[\![\mathbf{b}]\!]^L$ are calculated and shared to each party.
   Malicious: P_i shares to P_{i-1} and P_{i+1} respectively. Each party checks the copies they receive and aborts if an inconsistency is found.

To optimize neural networks in our experiments, we also use $\Pi_{\mathsf{MatMulMaxPoolReLU}}$, $\Pi_{\mathsf{MatMulBatchNormReLU}}$, constructed with minor changes in step 5) of Π_{ReLU}.

However, Π_{Softmax}, which is also one of the most frequently used protocols in deep learning, cannot be adapted in the same way due to the costly exponentiation operations.

4.5 Softmax

Exponentiation is an essential component of modern deep learning models. For example, logistic or softmax requires exponentiation. In this work, we focus on softmax, which is extensively used in modern models such as Transformers [71]. The way classical MPC [31, 51] realizes softmax leads to a large overhead due to two main reasons: 1. the complex protocol to approximate the exponentiation; 2. the max function to be applied before softmax. A recent study [70] shows that softmax is the main source of overhead when running a Transformer network with an MPC protocol and also introduces a numerical stability problem.

The Softmax on a vector $\mathbf{x}$ is defined as follows:

$$\mathsf{Softmax}(\mathbf{x}) := \exp(\mathbf{x}) / \sum_{i=1}^{n} \exp(\mathbf{x}_i) \tag{1}$$

In a regular ML setting, taking exponentiation over a value can easily lead to overflow, especially in a fixed-point representation, which MPC protocols need to use. The traditional solution to the overflow issue is to take the maximum of the input $\mathbf{x}$ and then subtract it from every element before feeding it into the softmax function. The risk of overflowing is

removed as the maximum input value would be 0. However, the extra max operation introduces an even more considerable overhead to an MPC protocol, as shown in the recent study [70].

A naïve extension of the previous protocol for exp would be to move exp to the LTEE, similar to the other non-linear operations in §4.2. This would not work due to the low computational power of the LTEE and the large amount of computation needed for exp compared to other operations. Under our assumption on the TEE hardware (details in §5, tests show that 1 million 32-bit multiplications take less than a second, while double-precision exponentiation takes over a minute). Unlike simple non-linear operations, exp needs to be done with floating point arithmetic for high precision, and each exp can involve tens of multiplications during the process. This approach will lead to significant overhead on a small LTEE, and introduce a new bottleneck for our scheme.

Our solution is to split and "offload" the computation to the untrusted local machine. The most complex part of the exp operation is performed by the powerful but untrusted CPU/GPU, and then the results are assembled within the LTEE. The main idea of the protocol is based on the fact that $\exp(a+b+c) = \exp(a)\exp(b)\exp(c)$, which implies that untrusted machines can complete exp on individual shares so that only simple multiplications are done inside of the LTEE. However, challenges remain to keep the protocol secure while also dealing with the conversion between fixed-point representations and real-number arithmetic. In Protocol 6, we expand the exponent part (see §3.1) to contain all possible results of

Protocol 5 $[\![\mathsf{ReLU}(\mathbf{A} \times \mathbf{B})]\!]^L \leftarrow \Pi_{\mathsf{MatMulReLU}}([\![\mathbf{A}]\!]^L, [\![\mathbf{B}]\!])$: Multiply $\mathbf{A}$ and $\mathbf{B}$, then output the shares of the ReLU of the results.

Input. $\{P_i\}$ have shares of $\mathbf{A} \in \mathbf{Z}_L^{a \times b}$ and $\mathbf{B} \in \mathbf{Z}_L^{b \times c}$.
Output. $\{P_i\}$ get shares of $[\![\mathbf{C}]\!]^L = [\![\mathsf{ReLU}(\mathbf{A} \times \mathbf{B})]\!]^L$.

1. P_1, P_2, and P_3 locally computes $[\![\hat{\mathbf{C}}]\!]_i^L = [\![\mathbf{A}]\!]_i^L \times [\![\mathbf{B}]\!]_i^L + [\![\mathbf{A}]\!]_i^L \times [\![\mathbf{B}]\!]_{i+1}^L + [\![\mathbf{A}]\!]_{i+1}^L \times [\![\mathbf{B}]\!]_i^L$.
   Malicious: Parties instead perform $\Pi_{\mathsf{mal\text{-}arith\text{-}mult}}$ of [44] to ensure that the multiplications (before truncation) were performed faithfully by parties. In the end, the 2-out-of-3 sharing $[\![\hat{\mathbf{C}}]\!]$ is distributed.

2. P_i calls H_i to execute $\Pi_{\mathsf{LTEE.GenMaskShare}}(a \times c, L)$ to obtain the masks $[\![\mathbf{M}]\!]_i \in \mathbf{Z}_L^{a \times c}$, then compute $\hat{\mathbf{C}}'_i = [\![\hat{\mathbf{C}}]\!]_i^L + [\![\mathbf{M}]\!]_i$. P_{i-1} also calls H_{i-1} to perform $\Pi_{\mathsf{LTEE.GenMaskShare}}(a \times c, L)$ to obtain $[\![\mathbf{M}]\!]_{i-1} \in \mathbf{Z}_L^{a \times c}$ and $\hat{\mathbf{C}}'_{i-1} = [\![\hat{\mathbf{C}}]\!]_{i-1}^L + [\![\mathbf{M}]\!]_{i-1}$.
   Malicious: Instead of doing the semi-honest protocol, P_i, P_{i-1} generates $[\![\mathbf{M}]\!]_i \leftarrow \Pi_{\mathsf{LTEE.GenMask}}(a \times c, L, i)$ and $\hat{\mathbf{C}}'_i = [\![\hat{\mathbf{C}}']\!]_i^L + [\![\mathbf{M}]\!]_i$. P_{i-1}, P_{i+1} also generates $[\![\mathbf{M}]\!]_{i+1}$ invoking $\Pi_{\mathsf{LTEE.GenMask'}}(a \times c, L, i-1)$, $\hat{\mathbf{C}}'_{i-1} = [\![\hat{\mathbf{C}}']\!]_{i-1}^L + [\![\mathbf{M}]\!]_{i+1}$.

3. P_i and P_{i-1} send $\hat{\mathbf{C}}'_i$ and $\hat{\mathbf{C}}'_{i-1}$ to P_{i+1}.
   Malicious: Instead of doing the semi-honest protocol, P_{i-1}, P_{i+1} send $\hat{\mathbf{C}}'_i$ to P_i, P_{i-1}, P_{i+1} send $\mathbf{C}'_{i-1}$ to P_i.

4. P_{i+1} computes $\hat{\mathbf{C}}' = \hat{\mathbf{C}}'_i + \hat{\mathbf{C}}'_{i-1} + [\![\hat{\mathbf{C}}']\!]_{i+1}^L$ and passes it to H_{i+1}.
   Malicious: Instead of doing the semi-honest protocol, P_i, P_{i+1} compare the two received copies and abort if inconsistency is found. P_{i+1} computes $\hat{\mathbf{C}}' = \hat{\mathbf{C}}'_i + [\![\hat{\mathbf{C}}]\!]_{i-1}^L + [\![\hat{\mathbf{C}}]\!]_{i+1}^L$ and passes it to H_{i+1}, P_i computes $\hat{\mathbf{C}}' = \hat{\mathbf{C}}'_{i-1} + [\![\hat{\mathbf{C}}]\!]_{i+1}^L + [\![\hat{\mathbf{C}}]\!]_i^L$ and passes it to H_i.

5. **LTEE Only** : H_{i+1} generates the masks $[\![\mathbf{M}]\!]_{i+1}$ by invoking $\Pi_{\mathsf{LTEE.GenMaskShare}}(a \times c, L)$ and recovers the plaintext through truncation: $\hat{\mathbf{C}} = \lfloor (\hat{\mathbf{C}}' + [\![\mathbf{M}]\!]_{i+1}) \rfloor \gg \mathsf{fp}$. Note that $[\![\mathbf{M}]\!]_{i+1} + [\![\mathbf{M}]\!]_i + [\![\mathbf{M}]\!]_{i-1} = \mathbf{0}$.
   Set $\mathbf{D} = (\mathbf{x} > \mathbf{0})$. Then H_{i+1} invokes $\Pi_{\mathsf{LTEE.GenMaskShare}}(a \times c, L)$ to get $[\![\mathbf{Z}^*]\!]_i^L \in \mathbb{Z}_L^{a \times c}$, $[\![\mathbf{Z}^*]\!]_{i+1}^L \in \mathbb{Z}_L^{a \times c}$, and compute: $([\![Z_{j,k}]\!]_i^L, [\![Z_{j,k}]\!]_{i+1}^L) = ((D_{j,k}?X_{j,k}:0) + [\![Z_{j,k}^*]\!]_i^L, [\![Z_{j,k}^*]\!]_{i+1}^L)$. Return them to P_{i+1}.
   P_i and P_{i-1} call H_i and H_{i-1} to invoke $\Pi_{\mathsf{LTEE.GenMaskShare}}(a \times c, L)$ to get $[\![\mathbf{Z}]\!]_{i-1}^L \in \mathbb{Z}_L^{a \times c}$.
   Malicious: Instead, H_{i+1} generates masks with $\Pi_{\mathsf{LTEE.GenMask}}(a \times c, L, i)$ to recover the plaintext $\hat{\mathbf{C}} = \lfloor (\hat{\mathbf{C}}' - [\![\mathbf{M}]\!]_{i+1}) \rfloor \gg \mathsf{fp}$, with the remaining being the same. H_i do as above respectively with index $i-1$ replacing index i, replacing $\Pi_{\mathsf{LTEE.GenMask}}$ with $\Pi'_{\mathsf{LTEE.GenMask}}$, and fix that the plaintext results are added to mask share i (i.e., the final $([\![Z_{j,k}]\!]_{i-1}^L, [\![Z_{j,k}]\!]_i^L) = ([\![Z_{j,k}]\!]_{i-1}^L, (D_{j,k}?X_{j,k}:0) + [\![Z_{j,k}^*]\!]_i^L))$. H_{i-1} and H_{i+1} also generate the remaining share for P_{i-1} and P_{i+1} respectively.

6. P_{i+1} send $[\![\mathbf{Z}]\!]_i^L, [\![\mathbf{D}]\!]_i^L$ to P_i, send $[\![\mathbf{Z}]\!]_{i+1}^L, [\![\mathbf{D}]\!]_{i+1}^L$ to P_{i-1}. Now, $[\![\mathbf{Z}]\!]^L$ and $[\![\mathbf{D}]\!]^L$ are calculated and shared with each party.
   Malicious: P_i shares $[\![\mathbf{Z}]\!]_{i-1}^L, [\![\mathbf{D}]\!]_{i-1}^L$ and $[\![\mathbf{Z}]\!]_i^L, [\![\mathbf{D}]\!]_i^L$ to P_{i-1} and P_{i+1} respectively. Each party checks the results from the parallel two computations and aborts if an inconsistency is found.

$\exp([\![x]\!]_i^L)$, specifically for $L = 2^{32}$. Overflow would not occur in our protocol after this adjustment, even without invoking max function before Softmax.

5 Evaluation

5.1 Experimental Setup

Implementation and baselines. We implemented STAMP in C++. As mentioned, our implementation is based on Falcon [68], keeping the basic MPC protocols, adding the new protocols, adding GPU supports for linear layers, and switching the networking library to ZeroMQ. Falcon is the main framework we compare to, but the open-source project was not implemented to support GPUs and does not address a key protocol for Transformers: Softmax. As a baseline, we extended Falcon and called this new baseline Falcon+, which includes three improvements over Falcon: 1. GPU support for linear layers, 2. a new MPC protocol for π_{softmax}, which is implemented using the exponentiation protocol of [31] combined with Π_{Div} and Π_{Max} provided by Falcon, 3. ZeroMQ

[75] as a networking library for better performance and fair comparison with the proposed scheme. These changes do not harm the threat model.

We also compare our scheme with AriaNN [57], but we use Falcon as the primary baseline for a few reasons. We found that Falcon and AriaNN are comparable; AriaNN shows benefits compared to Falcon in some settings, but also disadvantages in others before our optimizations for Falcon+. AriaNN also consumes a large amount of memory due to its technique, e.g., a server with 64GB DRAM can only support inputs of batch size 8 for ResNet18 inference, while 32GB is enough for batch size 128 in our case.

Hardware and network. We run our experiments on Cloudlab c240g5 machines over Ubuntu 20.04 LTS with an Intel Xeon Silver 4114 10-core CPU at 2.20 GHz and a NVIDIA 12GB P100 GPU. Our network setup is similar to previous studies [68, 67, 57, 45]: the LAN has 625 MBps bandwidth and around 0.2 ms ping. time, the WAN has 40 MBps bandwidth and 70 ms ping time. Both semi-honest and malicious settings are tested. For the LTEE-chip, we use Arduino Due with Atmel SAM3X8E ARM Cortex-M3 CPU (84MHz, 512

Protocol 6 $\Pi_{\mathsf{Softmax}}(\mathbf{x})$ compute softmax

Input. $\{P_i\}$ have replicative shares of $\mathbf{x} \in \mathbb{Z}_L^n$.

Output. $\{P_i\}$ get $[\![\exp(\mathbf{x})]\!]^L$

Initial values. The LTEEs save (q_L, m_L) for later use where $2^{q_L} \cdot (m_L \gg 52) = \exp(L \gg \mathsf{fp})$, $q_L \in \mathbb{Z}_{2^{32}}, m_L \in \mathbb{Z}_{2^{52}}, (m_L \gg 52), \in [0,1)$. fp is the fixed-point precision. We note $\bar{\mathbf{x}}$ to be the real values that $\mathbf{x}$ represents.

1. For each $[\![x_j]\!]^L$, P_i computes $\bar{r} = \overline{\exp([\![x_j]\!]_i^L \gg \mathsf{fp})}$. Let $\bar{r} = \overline{\exp([\![x_j]\!]_i^L \gg \mathsf{fp})} = 2^{q_j} \cdot (m_j \gg 52)$ where m_j has no sign since it is always positive). $(q_j = \lfloor \log_2(\exp([\![x_j]\!]_i^L \gg \mathsf{fp})) \rfloor = \lfloor \log_2(([\![x_j]\!]_i^L \gg \mathsf{fp}) \cdot \log_2(e)) \rfloor < 2^{32}$. We can see that 32 bits are enough to store q_j.

   Invoke $\Pi_{\mathsf{LTEE.GenMaskShare}}$ from H_i to generate two masks $\alpha_j \in \mathbb{Z}_{2^{52}}$ and $\beta_j \in \mathbb{Z}_{2^{32}}$ with the corresponding dimension (use truncation to match the dimensions), and send $\{m_j^* = (m_j + \alpha_j)_{2^{52}}, q_j^* = (q_j + \beta_j)_{2^{32}}\}$ for $i = 1,...,n$ to P_{i+1}.

   Malicious: P_{i-1} follows the same computation to get $\{m_j^*, q_j^*\}$ to P_{i+1}. P_{i-1}, P_{i+1} additionally compute $'\bar{r} = \overline{\exp([\![x_j]\!]_{i-1}^L \gg \mathsf{fp})}$ and obtain $\{'m_j^*, 'q_j^*\}$ by masking the mantissa and exponent part with masks from $\Pi'_{\mathsf{LTEE.GenMaskShare}}$, send them to P_i.

2. P_{i+1} receives $\{q_j^*, m_j^*\}$ and computes $2^{\hat{q}_j} \cdot \hat{m}_j := \overline{\exp(([\![x_j]\!]_{i-1}^L + [\![x_j]\!]_{i+1}^L)_L \gg \mathsf{fp})}$. Send $\{\mathbf{q}^* + \hat{\mathbf{q}}, \mathbf{m}^*, \hat{\mathbf{m}}\}$ to H_{i+1}.

   Malicious: P_i and P_{i+1} compare the two received copies and abort if an inconsistency is found. P_i do the same computation as above with index $i-1$ replacing index i, and send the obtained $\{'\mathbf{q}^* + '\hat{\mathbf{q}}, '\mathbf{m}^*, '\hat{\mathbf{m}}\}$ to H_i.

3. **LTEE Only**: H_{i+1} Generate α_j and β_j, Compute $q_j' = (q_j^* + \hat{q}_j) - \beta_j = q_j + \hat{q}_j$, $m_j' = (m_j^* - \alpha_j) \cdot \hat{m}_j = m_j \cdot \hat{m}_j$. Define the results $2^{\hat{q}_j'} \cdot m_j' := \overline{\exp([\![x_j]\!]_i^L \gg \mathsf{fp})} \cdot \overline{\exp(([\![x_j]\!]_{i-1}^L + [\![x_j]\!]_{i+1}^L)_L \gg \mathsf{fp})} = \overline{\exp((([\![x_j]\!]_{i-1}^L + [\![x_j]\!]_{i+1}^L)_L + [\![x_j]\!]_i^L) \gg \mathsf{fp})}$

   For the fixed-point representation $x_j \in [0, L)$, the real value it represents $\bar{x}_j \in [-L/2 \gg \mathsf{fp}, L/2 \gg \mathsf{fp})$, $\lceil \log_2(\exp(x)) \rceil \in [-(L/2) \gg \mathsf{fp} \cdot \log_2(e), (L/2) \gg \mathsf{fp} \cdot \log_2(e)]$. Set the q-bound: $\mathsf{qb} = ((L/2) \gg \mathsf{fp}) \cdot \log_2(e)$. Define $\overline{\exp(\bar{x}_j)} := 2^{q_j''} \cdot (m_j'' \gg 52)$, then q_j'' should be in $[-\mathsf{qb}, \mathsf{qb}]$.

   q_j' and m_j' may alter from the correct q_j'' and m_j'' for two possible reasons: We are missing an L to be subtracted if $([\![x_j]\!]_{i-1}^L + [\![x_j]\!]_{i+1}^L)_L + [\![x_j]\!]_i^L \neq ([\![x_j]\!]_i^L + [\![x_j]\!]_{i+1}^L + [\![x_j]\!]_{i-1}^L)_L = x_j$; or $\bar{x}_j$, or the real value x_j represents is actually negative, so $\bar{x}_j = (([\![x_j]\!]_i^L + [\![x_j]\!]_{i+1}^L + [\![x_j]\!]_{i-1}^L)_L - L) \gg \mathsf{fp}$. H_{i+1} runs:

   (a) If $q_j' \in (0, \mathsf{qb}]$, $q_j'' = q_j'$, $m_j'' = m_j'$.

   (b) If $q_j' \in (\mathsf{qb}, 3 * \mathsf{qb}]$, we are missing one $\exp(-L \gg \mathsf{fp})$ to be multiplied for either reason. Compute $q_j'' = q_j' - q_L$, $m_j'' = (m_j^* - \alpha_j) \cdot \hat{m}_j / m_L$.

   (c) If $q_j' \in (3 * \mathsf{qb}, 5 * \mathsf{qb}]$, we are missing $\exp(-2L \gg \mathsf{fp})$ to be multiplied for both reasons. Compute $q_j'' = q_j' - 2 * q_L$, $m_j'' = (m_j^* - \alpha_j) \cdot \hat{m}_j / (m_L)^2$.

   Now H_{i+1} obtains the corrected $\exp(\bar{x}_j) = 2^{q_j''}(m_j'' \gg 52)$. H_{i+1} then compute softmax of the real values directly by $\mathsf{Softmax}(\bar{\mathbf{x}}) = \exp(\bar{\mathbf{x}}) / \sum(\exp(\bar{\mathbf{x}}))$ which involves only $O(n)$ additions, $O(1)$ multiplications and divisions. Then convert the results to fixed-point representations, and invoke $\Pi_{\mathsf{LTEE.GenMaskShare}}$ for masks $[\![\mathbf{m}]\!]_{i+1}^L, [\![\mathbf{m}]\!]_{i-1}^L$ to output $([\![\mathbf{y}]\!]_{i+1}^L, [\![\mathbf{y}]\!]_{i-1}^L) = (\mathsf{Softmax}(\mathbf{x}) + [\![\mathbf{m}]\!]_{i+1}^L, [\![\mathbf{m}]\!]_{i-1}^L)$ to P_{i+1}.

   P_i and P_{i-1} call H_i and H_{i-1} to generate $[\![\mathbf{m}]\!]_i^L = \Pi_{\mathsf{LTEE.GenMaskShare}}(n)$ as $[\![\mathbf{y}]\!]_i^L$.

   Malicious: H_i do the computation accordingly, replacing $\Pi_{\mathsf{LTEE.GenMaskShare}}$ with $\Pi'_{\mathsf{LTEE.GenMaskShare}}$, while also masking the results with the index masks i. P_{i-1} and P_{i+1} call H_{i-1} and H_{i+1} to generate $[\![\mathbf{m}]\!]_{i-1}^L = \Pi'_{\mathsf{LTEE.GenMaskShare}}(n, L)$ as $[\![\mathbf{y}]\!]_{i-1}^L$.

4. P_{i+1} share $[\![\mathbf{y}]\!]_{i+1}^L$ with P_i and $[\![\mathbf{y}]\!]_{i-1}^L$ with P_{i-1}

   Malicious: P_i shares $[\![\mathbf{y}]\!]_i^L$ to P_{i-1} and $[\![\mathbf{y}]\!]_{i+1}^L$ to P_{i+1} respectively. Each party checks the results of the two parallel computations and aborts if an inconsistency is found.

KB of Flash and up to 100 KB of SRAM), which is used for a commercial TPM implementation [63], to evaluate the LTEE runtime. We also assume that the LTEE has the low-pin-count (LPC) bus (same as a TPM), which leads to a 15MBps bandwidth limit in our experiments. The capability of a TPM to generate random numbers will not meet our need for throughput. As shown in [60], a maximum of 3MB/s of generation can be achieved in a TPM, which is enough for its original

use case, but not for our scheme. We assume that a low-cost hardware AES engine [11] is added, and its throughput of 14 GBps makes the LTEE's pseudo-random number generation time negligible compared to the data transmission time through the low bandwidth interconnect. Other details of the hardware can be seen in §5.4. For the SoC LTEE, we assume the same Cortex-M3 processor running at 1GHz and the 128-bit on-chip network (16GBps). The performance is estimated

by scaling the execution time of the discrete LTEE.

Neural networks and Dataset. We use 8 neural networks: a small 3-layer fully-connected network with ReLU activations (Network-A, as in SecureML [45]), a small convolutional network with ReLU activation (Network-B, as in [54]), a small convolutional network with ReLU activation and max-pooling (Network-C, as in [38]), AlexNet [33], VGG16 [59], ResNet18 [21] and a small Transformer [66]. We pick the small Transformer network with limited dimensions and a small number of multi-head attention due to the fact that Softmax is too expensive in pure MPC for a reasonable evaluation time, especially in a WAN setting. The input data sets are MNIST [10] for the first four networks, CIFAR-10 [32] for AlexNet and VGG16, ImageNet [56] for ResNet18, and Wikitext-2 [42] for the Transformer.

Parameter choice. As mentioned in §4.5, we choose $L = 2^{32}$ and fp = 13 in our implementation. We pick the group size to be 1024 bits in Diffie–Hellman key exchange and use AES-128 for the pseudo-random number generation.

5.2 Performance

Table 1 and Table 2 show the end-to-end latency (in seconds) of the inference on inputs of batch size 128 in semi-honest and malicious settings, respectively. Table 3 and Table 4 report the amount of data transmitted. '-' in the cells indicates that the implementation is missing or the network is too large for CPU evaluation. AriaNN does not implement its work in a malicious setting.

In the tables, we compare STAMP with Falcon [68] and AriaNN [57], two of the state-of-the-art MPC frameworks. AriaNN does not implement the execution of different parties on separate machines, but instead uses the local simulation of the network for performance evaluation. Depending on the structure of the machine learning network, STAMP with LTEE-chip is 4× to 63× or 6× to 59× faster than the state-of-the-art MPC results with semi-honest or malicious settings in WAN / GPU environments. The advantage that we obtain under a LAN or CPU environment is smaller compared to a WAN/GPU environment. In the LAN, communication overhead is significantly reduced. With a CPU, the computation accounts for a larger portion of the execution time. These factors reduce the speedup, which is mainly accomplished by reducing the communication overhead of non-linear functions. STAMP with LTEE-SoC achieves even higher speedup, and compared to STAMP with LTEE-chip, the gap is the largest in LAN / GPU environments where local communication overhead is large. Also, note that for smaller networks, a GPU is sometimes slower than a CPU. For a small amount of data and a small deep learning model, initialization and data movement may take more time than operating directly on a CPU. For larger models, the improvement with a GPU is more consistent.

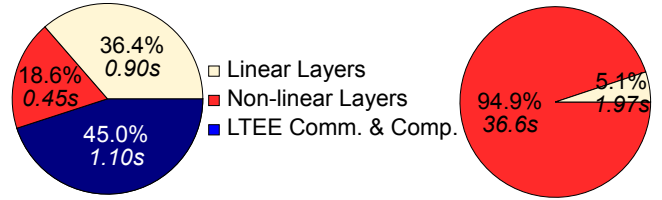To study the effect of STAMP on execution time breakdown,

Figure 3: The breakdown of local machine execution time: linear layers, non-linear layers, and LTEE bus communication & computation time. STAMP (left) and Falcon+ (right) on semi-honest inference over AlexNet under WAN/GPU.

in Figure 3 we show the time breakdown of semi-honest inference over AlexNet under the WAN/GPU setting. In both STAMP and Falcon+, linear layers, including convolution layers and fully-connected layers with almost the same protocols, take a similar amount of time. However, they contribute only 5.1% of the total execution time in Falcon+, and over 36% in STAMP, because the non-linear layers' runtime is significantly reduced from about 94.9% to 18.6% (63.6% if we roughly consider all operations on the LTEE are related to non-linear layers. There is some overhead, such as the local transmission in step 4 of Protocol 5, which cannot be assigned to be only linear or non-linear operations). We also show in Table 5 another breakdown of the execution time in the WAN/GPU setting: CPU/GPU, communication, and LTEE. Note that we are moving major parts of the computation of most non-linear operations to the LTEE, so the CPU/GPU execution time is reduced compared with Falcon+.

STAMP trades off the interparty communication with the local communication between LTEE and the untrusted CPU/GPU. However, as can be seen in Table 3 and Table 4, for LTEE-chip, the low (15 MBps) bus bandwidth becomes one of the bottlenecks of our performance with large networks, especially in the LAN setting. In Table 3, more than 3GB of data is transmitted through the bus for the ResNet18 reference, causing more than 200 seconds of communication time, which is about 60% of the total execution time of our scheme. LTEE-SoC provides much higher LTEE-CPU bandwidth and significantly alleviate this bottleneck.

Figure 4) shows how the speedup over Falcon+ can change if we use a higher-bandwidth interconnect for the LTEE. In this figure, we choose two computation-heavy networks, VGG16 and ResNet18, and a communication-heavy Transformer network (due to frequently used Softmax) as examples. We can observe a considerable boost in performance with a higher LTEE bandwidth.

Pure CPU TEE Solution. We also obtain the results achieved by a pure TEE solution as a reference. The pure SGX experiment assumes that semi-honest parties can securely share their data to one party's SGX for evaluation and is executed on SGX V1 with 16GB enclave memory on Azure

| | Network-A | | | | Network-B | | | | Network-C | | | |
Framework	LAN GPU	LAN CPU	WAN GPU	WAN CPU	LAN GPU	LAN CPU	WAN GPU	WAN CPU	LAN GPU	LAN CPU	WAN GPU	WAN CPU
Falcon+	0.0824	0.1118	1.478	1.393	0.2034	0.2618	1.464	1.292	1.866	2.191	7.321	7.288
AriaNN	0.2560	0.5120	-	5.504	-	-	-	-	3.072	5.248	-	17.02
STAMP-chip	**0.0737**	**0.0777**	**0.2516**	**0.2946**	**0.1172**	**0.1142**	**0.2787**	**0.2938**	**0.6809**	**1.298**	**1.024**	**1.494**
speed-up	1.11×	1.43×	5.87×	4.72×	1.73×	2.29×	5.25×	4.39×	2.74×	1.68×	7.14×	4.87×
STAMP-SoC	0.0432	0.0472	0.2211	0.2641	0.0643	0.0613	0.1994	0.2408	0.1990	0.8163	0.5424	1.012
speed-up	1.91×	2.37×	6.69×	5.28×	3.17×	4.28×	7.34×	5.37×	9.38×	3.10×	13.5×	7.20×

| | LeNet | | | | AlexNet | | | | Transformer | | | |
Framework	LAN GPU	LAN CPU	WAN GPU	WAN CPU	LAN GPU	LAN CPU	WAN GPU	WAN CPU	LAN GPU	LAN CPU	WAN GPU	WAN CPU
Falcon+	2.592	4.603	8.867	9.563	4.276	11.78	38.56	43.06	4.026	-	321.0	-
AriaNN	4.480	7.040	-	18.30	9.984	19.20	-	43.52	-	-	-	-
STAMP-chip	**0.9693**	**3.075**	**1.315**	**3.255**	**1.564**	**9.263**	**2.463**	**9.449**	**0.5130**	-	**5.024**	-
speed-up	2.67×	1.49×	6.74×	2.93×	2.73×	1.27×	15.6×	4.55×	7.84×	-	63.8×	-
STAMP-SoC	0.2869	2.392	0.6328	2.573	0.3055	8.029	1.229	8.215	0.3618	-	4.873	-
speed-up	9.04×	2.02×	14.0×	3.72×	14.0×	1.52×	31.3×	5.24×	11.1×	-	65.8×	-

| | VGG16 | | | | ResNet18 | | | |
Framework	LAN GPU	LAN CPU	WAN GPU	WAN CPU	LAN GPU	LAN CPU	WAN GPU	WAN CPU
Falcon+	49.36	-	122.1	-	545.9	-	1439	
AriaNN*	198.4	-	-	-	1779	-	-	-
STAMP-chip	**26.55**	-	**30.05**	-	**309.7**	-	**350.7**	-
speed-up	1.85×	-	4.06×	-	1.76×	-	4.10×	-
STAMP-SoC	13.06	-	16.56	-	106.9	-	148.0	-
speed-up	3.78×	-	7.37×	-	5.10×	-	9.72×	-

Table 1: Inference time (s) of a 128 batch in a semi-honest setting. AriaNN has a reduced batch size of 64 and 8 for VGG16 and ResNet18 due to memory consumption, which also applies to other tables.
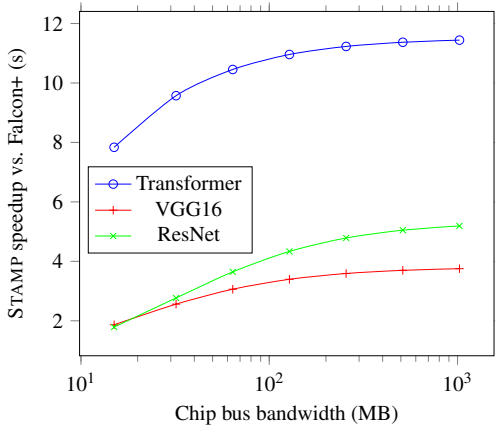

Figure 4: The speedup with different bus bandwidth in the semi-honest setting under LAN/GPU

Standard DC4s v3. Although for smaller networks such as Network-B, SGX performs slightly worse, 0.46 seconds compared to 0.12 of STAMP, mostly due to initialization, for larger networks such as ResNet18, Intel SGX only takes 8.15 seconds, while STAMP (LTEE-SoC) takes 148 second. This is expected as the TEE-only solution has no communication overhead. However, as discussed in §3.3, high-performance TEEs will be more difficult to secure compared to a small LTEE. The complete table is shown in Appendix E.

5.3 Accuracy

The precision of the inference using the plaintext computation and model weights is shown in Table 6, where the model weights are from the plaintext training. For Network-A, B, C and LeNet, which are measured by Falcon [68], STAMP has the same accuracy that Falcon achieved. STAMP optimizes overhead, but not computation precision, and we use the same size L of a finite field and the same fixed-point precision. In most schemes, for each batch of 128 elements, only one more sample would be classified incorrectly compared with the plaintext results, mainly due to the quantization when representing data in fixed-point precision. However, this simple transfer from a plaintext model to a fixed-point scheme may not work well in certain circumstances. If a portion of weights and activations break the range that fix-point representations can represent, the inference accuracy may degrade more significantly. Carefully capping the values during plaintext training can potentially avoid this issue.

Table 2 (first block):

Framework	Network-A				Network-B				Network-C			
	LAN GPU	LAN CPU	WAN GPU	WAN CPU	LAN GPU	LAN CPU	WAN GPU	WAN CPU	LAN GPU	LAN CPU	WAN GPU	WAN CPU
Falcon+	0.1921	0.3293	3.359	3.3701	0.6279	0.6416	3.504	3.0743	5.639	6.758	23.26	20.8988
Stamp-chip	**0.0913**	**0.2567**	**0.5150**	**0.7307**	**0.1594**	**0.2860**	**0.5803**	**0.7246**	**1.157**	**3.661**	**2.196**	**4.258**
speed-up	2.10×	1.51×	6.52×	4.61×	3.94×	2.82×	6.04×	4.24×	4.87×	2.12×	10.6×	4.91×
Stamp-SoC	0.0200	0.1854	0.4437	0.6594	0.0357	0.1623	0.4566	0.6010	0.0325	2.536	1.071	3.134
speed-up	9.59×	2.09×	7.57×	5.11×	17.5×	4.98×	7.67×	5.12×	173×	3.06×	21.7×	6.67×

Framework	LeNet				AlexNet				Transformer			
	LAN GPU	LAN CPU	WAN GPU	WAN CPU	LAN GPU	LAN CPU	WAN GPU	WAN CPU	LAN GPU	LAN CPU	WAN GPU	WAN CPU
Falcon+	7.492	15.38	28.82	32.57	13.89	41.88	100.9	123.2	10.99	-	777.9	-
Stamp-chip	**2.106**	**10.64**	**2.929**	**10.80**	**3.653**	**36.80**	**5.538**	**36.10**	**2.073**	-	**13.03**	-
speed-up	3.56×	1.55×	9.84×	3.01×	3.80×	1.27×	18.2×	3.41×	5.30×	-	59.6×	-
Stamp-SoC	0.5136	9.052	1.337	9.213	0.7738	33.92	2.659	33.22	1.720	-	12.68	-
speed-up	14.5×	1.82×	21.5×	3.54×	17.9×	1.37×	37.9×	3.71×	6.39×	-	61.3×	-

Framework	VGG16				ResNet18			
	LAN GPU	LAN CPU	WAN GPU	WAN CPU	LAN GPU	LAN CPU	WAN GPU	WAN CPU
Falcon+	136.9	-	407.8	-	1550	-	4993	-
Stamp-chip	**51.54**	-	**68.09**	-	**639.3**	-	**772.2**	-
speed-up	2.66×	-	5.99×	-	2.43×	-	6.47×	-
Stamp-SoC	20.06	-	36.62	-	166.2	-	299.1	-
speed-up	6.82×	-	11.1×	-	9.33×	-	16.6×	-

Table 2: Inference time (s) of a 128 batch in a malicious setting. AriaNN does not implement their work in a malicious setting.

Framework		Network-A	Network-B	Network-C	LeNet	AlexNet	Transformer	VGG16	ResNet18
Falcon+	Inter-party	1.536	6.272	64.87	95.33	173.5	72.21	1730	22933
AriaNN	Inter-party	2.816	-	38.54	55.04	121.6	-	1161	18944
Stamp	Inter-party	0.2058	0.8371	5.328	7.931	12.31	19.21	187.7	2106
	LTEE-CPU	0.4585	0.7958	7.235	10.24	18.53	2.270	202.5	3044

Table 3: Inference communication(MB) of a 128 batch in a semi-honest setting.

5.4 Lightweight TEE Hardware Overhead

The LTEE in Stamp consists of two parts:

1. The microcontroller with the same capability as a TPM, which executes computation (non-linear operations) - We refer to the design of ST33TPM12SPI as a baseline with $0.40mm^2$ area for the ARM SecurCore SC300, and the detailed parameters can be found on the product page [63]. It will be responsible for most protocols. The peak power consumption of the kernel is about $12mW$.

2. An AES engine performing pseudo-random number generation - A previous study [11] reports a cost of $0.13mm^2$ and $56mW$ in area and peak power consumption. The AES engine serves as the pseudo-random function F in $\Pi_{\text{LTEE.GenMask}}$ and $\Pi_{\text{LTEE.GenMaskShare}}$.

The combined overhead of $0.53mm^2$ and $68mW$ is quite small, suggesting that LTEE represents a lightweight solution, which is cheaper and easier to deploy compared to adding a TEE to a high-performance processor. LTEE can even become a simple extension of the existing TPM or the on-chip SoC security subsystem. Furthermore, because LTEE-chip can be built independently of the main compute engines such as CPUs, GPUs, and accelerators, our protocol can be deployed with existing or future hardware platforms without integrating new TEE features directly into them. We note that the LTEE overhead here does not represent the full power consumption of Stamp, which also need to run an MPC protocol on an untrusted CPU/GPU.

6 Related Work

Privacy-preserving inference. Privacy-preserving inference has been extensively studied in recent years. Cryptographic techniques such as garbled circuits [7, 55], secret sharing [57, 44, 67], homomorphic encryption [45, 76] have been applied for privacy-preserving inference. Gazelle and Delphi [27, 43] combine homomorphic encryption and garbled cir-

Framework		Network-A	Network-B	Network-C	LeNet	AlexNet	Transformer	VGG16	ResNet18
Falcon+	Inter-party	10.51	41.33	423.4	620.1	1135	340.0	11543	139287
STAMP	Inter-party	0.8443	2.0704	21.02	28.80	48.68	131.2	838.6	7500
	LTEE-CPU	1.070	1.856	16.88	23.90	43.23	5.296	472.5	7103

Table 4: Inference communication (MB) of a 128 batch in a malicious setting.

Framework	Component	Network-A		Network-B		Network-C		LeNet		AlexNet		Transformer		VGG16		ResNet18	
		Time	Ratio	Time	Ratio	Time	Ratio	Time	Ratio	Time	Ratio	Time	Ratio	Time	Ratio	Time	Ratio
STAMP	CPU/GPU	0.04	17%	0.06	23%	0.19	19%	0.28	21%	0.29	12%	0.30	6%	12.8	43%	98.0	28%
	Comm.	0.18	70%	0.16	58%	0.35	34%	0.35	27%	0.94	38%	4.56	91%	3.34	11%	44.0	13%
	LTEE	0.03	13%	0.05	19%	0.48	47%	0.68	52%	1.24	50%	0.16	3%	13.8	46%	207	59%
Falcon+	CPU/GPU	0.08	6%	0.20	14%	1.80	25%	2.50	28%	4.09	11%	3.95	1%	47.6	39%	523	36%
	Comm.	1.40	94%	1.27	86%	5.52	75%	6.37	72%	34.4	89%	317	99%	74.4	61%	916	64%

Table 5: Inference time (s) breakdown of a 128 batch in a semi-honest WAN/GPU setting, comparing with Falcon+.

Network	Plaintext Accuracy	STAMP Accuracy
Network-A	98.18%	97.42%
Network-B	98.93%	97.81%
Network-C	99.16%	98.64%
LeNet	99.76%	99.15%
ResNet18@1	84.76%	84.37%
ResNet18@5	95.80%	95.50%

Table 6: Accuracy on different networks. The weights of ResNet18 are from Torchvision [41].

cuits for their advantages in linear and non-linear operations, respectively. Falcon [68] implements a 3-party malicious secure protocol, combining techniques from SecureNN [67] and ABY3 [44]. Blaze [48] achieves not only 3-party malicious security but also fairness in an honest majority setting. AriaNN [57] leverages function secret sharing to reduce the communication rounds for specific functions, but at the cost of increasing the total amount of communication data in some cases. CrypTen [31] provides a general software framework that makes secure MPC primitives more easily used by integrating them into a popular ML framework, PyTorch.

A recent study [53] investigated a floating-point 2-party MPC to improve accuracy. Although we also discussed floating-point arithmetic in our protocol (§4.5), we only use floating-point operations for exponentiation assisted by LTEE.

Trusted hardware-assisted secure computation. Crypt-Flow [34] is based on MPC (secureNN), but it also leverages a TEE's integrity protection to achieve malicious security. Another work [18] proposes to split the secure computation between garbled circuits and trusted hardware (Intel SGX). OblivML [47] focuses on data-oblivious computation ML algorithms on SGX to prevent side-channel attacks. Iron [13] uses SGX to realize faster functional encryption, allowing authorized entities to perform selective computation on the encrypted data. Bahmani et al. [2] propose an offloading scheme for Intel SGX to solve the MPC with the so-called "labeled attested computation". [77] introduces a two-party TEE aided MPC scheme, but mostly only focus on improving multiplication overhead; [46] as one of the newest work also manages to improve secure computation with DP, but it focuses on a local setting where no crypto methods are involved.

Large deep learning models are often run on GPUs for performance and energy efficiency. Slalom [62] and Darknight [20] propose to run a private computation on an untrusted GPU by securely offloading linear operations from the CPU TEE (SGX) to the GPU using secret sharing. However, these approaches still require the CPU TEE to perform a significant amount of computation for linear operations and are also limited by the amount of secure memory provided by SGX. STAMP, on the other hand, only requires a small low-performance TEE for non-linear operations by protecting linear operations on untrusted CPUs/GPUs with the MPC.

Some applications other than MPC include FastBFT [39] which introduces a low message complexity byzantine fault-tolerant protocol with the help of SGX. EnclaveDB [50] achieves a 100x smaller TCB compared to a conventional database server by storing sensitive data within an enclave.

Unfortunately, complex modern processors are vulnerable to timing-channel attacks, and similar attacks have been demonstrated for the TEEs on high-performance processors in recent years [65, 64, 17]. These attacks can be mitigated by carefully designing algorithms and software inside a TEE, but such mitigation requires nontrivial efforts and may not be able to prevent attacks completely. We believe that STAMP is the first to combine a small TEE chip with MPC for privacy-preserving machine learning, introducing a new trade-off point between security and performance.

7 Conclusion and Future Works

This paper introduces a new MPC protocol for private machine learning, which significantly reduces the overhead of MPC with the assistance of a lightweight TEE. The protocol can guarantee security against corrupted parties with malicious behavior in an honest-majority 3-party setting. We provide theoretical analysis and experiment results to show that STAMP achieves orders of magnitude higher performance over state-of-the-art MPC protocols in various environments, even with a tiny TEE chip whose capability is comparable to a TPM.

References

[1] *Azure Machine Learning Studio*. https://azure.microsoft.com/en-us/services/machine-learning/.

[2] Raad Bahmani et al. "Secure multiparty computation from SGX". In: *International Conference on Financial Cryptography and Data Security*. Springer. 2017, pp. 477–497.

[3] Alexander Sprogø Banks, Marek Kisiel, and Philip Korsholm. "Remote attestation: a literature review". In: *arXiv preprint arXiv:2105.02466* (2021).

[4] Ferdinand Brasser et al. "Software grand exposure:SGX cache attacks are practical". In: *11th USENIX Workshop on Offensive Technologies (WOOT 17)*. 2017.

[5] Ran Canetti. "Security and composition of multiparty cryptographic protocols". In: *Journal of CRYPTOLOGY* 13.1 (2000), pp. 143–202.

[6] Ran Canetti. "Universally composable security: A new paradigm for cryptographic protocols". In: *Proceedings 42nd IEEE Symposium on Foundations of Computer Science*. IEEE. 2001, pp. 136–145.

[7] Nishanth Chandran et al. "EzPC: programmable, efficient, and scalable secure two-party computation for machine learning". In: *Cryptology ePrint Archive* (2017).

[8] Joseph I Choi et al. "A hybrid approach to secure function evaluation using SGX". In: *Proceedings of the 2019 ACM Asia Conference on Computer and Communications Security*. 2019, pp. 100–113.

[9] Victor Costan and Srinivas Devadas. "Intel SGX explained". In: *Cryptology ePrint Archive* (2016).

[10] Li Deng. "The mnist database of handwritten digit images for machine learning research". In: *IEEE Signal Processing Magazine* 29.6 (2012), pp. 141–142.

[11] Pham-Khoi Dong, Hung K Nguyen, and Xuan-Tu Tran. "A 45nm high-throughput and low latency aes encryption for real-time applications". In: *2019 19th International Symposium on Communications and Information Technologies (ISCIT)*. IEEE. 2019, pp. 196–200.

[12] Susanne Felsen et al. "Secure and private function evaluation with Intel SGX". In: *Proceedings of the 2019 ACM SIGSAC Conference on Cloud Computing Security Workshop*. 2019, pp. 165–181.

[13] Ben Fisch et al. "Iron: functional encryption using Intel SGX". In: *Proceedings of the 2017 ACM SIGSAC Conference on Computer and Communications Security*. 2017, pp. 765–782.

[14] Jun Furukawa et al. "High-throughput secure three-party computation for malicious adversaries and an honest majority". In: *Annual international conference on the theory and applications of cryptographic techniques*. Springer. 2017, pp. 225–255.

[15] Oded Goldreich, Silvio Micali, and Avi Wigderson. "How to play any mental game, or a completeness theorem for protocols with honest majority". In: *Providing Sound Foundations for Cryptography: On the Work of Shafi Goldwasser and Silvio Micali*. 2019, pp. 307–328.

[16] *Google Cloud AI*. https://cloud.google.com/products/machine-learning/.

[17] Johannes Götzfried et al. "Cache attacks on Intel SGX". In: *Proceedings of the 10th European Workshop on Systems Security*. 2017, pp. 1–6.

[18] Debayan Gupta et al. "Using intel software guard extensions for efficient two-party secure function evaluation". In: *International Conference on Financial Cryptography and Data Security*. Springer. 2016, pp. 302–318.

[19] Jago Gyselinck et al. "Off-limits: Abusing legacy x86 memory segmentation to spy on enclaved execution". In: *International Symposium on Engineering Secure Software and Systems*. Springer. 2018, pp. 44–60.

[20] Hanieh Hashemi, Yongqin Wang, and Murali Annavaram. "Darknight: A data privacy scheme for training and inference of deep neural networks". In: *arXiv preprint arXiv:2006.01300* (2020).

[21] Kaiming He et al. "Deep residual learning for image recognition". In: *Proceedings of the IEEE conference on computer vision and pattern recognition*. 2016, pp. 770–778.

[22] Weizhe Hua et al. "Guardnn: Secure dnn accelerator for privacy-preserving deep learning". In: *arXiv preprint arXiv:2008.11632* (2020).

[23] Apple Inc. *Apple Secure Enclave*. URL: https://support.apple.com/guide/security/secure-enclave-sec59b0b31ff/web (visited on 10/03/2022).

[24] Google Inc. *Google Titan Key*. URL: https://cloud.google.com/titan-security-key/ (visited on 10/03/2022).

[25] Qualcomm Incorporated. *Qualcomm Secure Processing Unit*. URL: https://www.qualcomm.com/news/releases/2019/06/qualcomm-snapdragon-855-becomes-first-mobile-soc-receive-smart-card (visited on 10/03/2022).

[26] Rambus Incorporated. *RT-630 Programmable Root of Trust*. URL: https://www.rambus.com/security/root-of-trust/rt-630/ (visited on 10/03/2022).

[27] Chiraag Juvekar, Vinod Vaikuntanathan, and Anantha Chandrakasan. "GAZELLE: A low latency framework for secure neural network inference". In: *27th USENIX Security Symposium (USENIX Security 18)*. 2018, pp. 1651–1669.

[28] William Kahan. "IEEE standard 754 for binary floating-point arithmetic". In: *Lecture Notes on the Status of IEEE* 754.94720-1776 (1996), p. 11.

[29] Georgios Kaissis et al. "End-to-end privacy preserving deep learning on multi-institutional medical imaging". In: *Nature Machine Intelligence* 3.6 (2021), pp. 473–484.

[30] Jonathan Katz. "Universally composable multi-party computation using tamper-proof hardware". In: *Annual International Conference on the Theory and Applications of Cryptographic Techniques*. Springer. 2007, pp. 115–128.

[31] B. Knott et al. "CrypTen: Secure Multi-Party Computation Meets Machine Learning". In: *arXiv 2109.00984*. 2021.

[32] Alex Krizhevsky, Vinod Nair, and Geoffrey Hinton. "The CIFAR-10 dataset". In: *online: http://www.cs.toronto.edu/kriz/cifar.html* 55.5 (2014).

[33] Alex Krizhevsky, Ilya Sutskever, and Geoffrey E Hinton. "Imagenet classification with deep convolutional neural networks". In: *Advances in neural information processing systems* 25 (2012).

[34] Nishant Kumar et al. "Cryptflow: Secure tensorflow inference". In: *2020 IEEE Symposium on Security and Privacy (SP)*. IEEE. 2020, pp. 336–353.

[35] Dayeol Lee et al. "Keystone: An open framework for architecting trusted execution environments". In: *Proceedings of the Fifteenth European Conference on Computer Systems*. 2020, pp. 1–16.

[36] Jaehyuk Lee et al. "Hacking in darkness: Return-oriented programming against secure enclaves". In: *26th USENIX Security Symposium (USENIX Security 17)*. 2017, pp. 523–539.

[37] Sangho Lee et al. "Inferring fine-grained control flow inside SGX enclaves with branch shadowing". In: *26th USENIX Security Symposium (USENIX Security 17)*. 2017, pp. 557–574.

[38] Jian Liu et al. "Oblivious neural network predictions via minionn transformations". In: *Proceedings of the 2017 ACM SIGSAC conference on computer and communications security*. 2017, pp. 619–631.

[39] Jian Liu et al. "Scalable byzantine consensus via hardware-assisted secret sharing". In: *IEEE Transactions on Computers* 68.1 (2018), pp. 139–151.

[40] Yibiao Lu et al. "Correlated Randomness Teleportation via Semi-trusted Hardware—Enabling Silent Multi-party Computation". In: *European Symposium on Research in Computer Security*. Springer. 2021, pp. 699–720.

[41] Sébastien Marcel and Yann Rodriguez. "Torchvision the machine-vision package of torch". In: *Proceedings of the 18th ACM international conference on Multimedia*. 2010, pp. 1485–1488.

[42] Stephen Merity et al. "Pointer sentinel mixture models". In: *arXiv preprint arXiv:1609.07843* (2016).

[43] Pratyush Mishra et al. "Delphi: A cryptographic inference service for neural networks". In: *29th USENIX Security Symposium (USENIX Security 20)*. 2020, pp. 2505–2522.

[44] Payman Mohassel and Peter Rindal. "ABY3: A mixed protocol framework for machine learning". In: *Proceedings of the 2018 ACM SIGSAC conference on computer and communications security*. 2018, pp. 35–52.

[45] Payman Mohassel and Yupeng Zhang. "Secureml: A system for scalable privacy-preserving machine learning". In: *2017 IEEE symposium on security and privacy (SP)*. IEEE. 2017, pp. 19–38.

[46] Yue Niu, Ramy E Ali, and Salman Avestimehr. "3LegRace: Privacy-Preserving DNN Training over TEEs and GPUs". In: *Proceedings on Privacy Enhancing Technologies* 4 (2022), pp. 183–203.

[47] Olga Ohrimenko et al. "Oblivious Multi-Party Machine Learning on Trusted Processors". In: *25th USENIX Security Symposium (USENIX Security 16)*. 2016, pp. 619–636.

[48] Arpita Patra and Ajith Suresh. "BLAZE: blazing fast privacy-preserving machine learning". In: *arXiv preprint arXiv:2005.09042* (2020).

[49] Siani Pearson and Boris Balacheff. *Trusted computing platforms: TCPA technology in context*. Prentice Hall Professional, 2003.

[50] Christian Priebe, Kapil Vaswani, and Manuel Costa. "EnclaveDB: A secure database using SGX". In: *2018 IEEE Symposium on Security and Privacy (SP)*. IEEE. 2018, pp. 264–278.

[51] Prashanthi Ramachandran et al. "S++: A fast and deployable secure-computation framework for privacy-preserving neural network training". In: *arXiv preprint arXiv:2101.12078* (2021).

[52] Wolfgang Rankl and Wolfgang Effing. *Smart card handbook*. John Wiley & Sons, 2004.

[53] Deevashwer Rathee et al. "SecFloat: Accurate Floating-Point meets Secure 2-Party Computation". In: *Cryptology ePrint Archive* (2022).

[54] M Sadegh Riazi et al. "Chameleon: A hybrid secure computation framework for machine learning applications". In: *Proceedings of the 2018 on Asia conference on computer and communications security*. 2018, pp. 707–721.

[55] M Sadegh Riazi et al. "XONN:XNOR-based Oblivious Deep Neural Network Inference". In: *28th USENIX Security Symposium (USENIX Security 19)*. 2019, pp. 1501–1518.

[56] Olga Russakovsky et al. "ImageNet Large Scale Visual Recognition Challenge". In: *International Journal of Computer Vision (IJCV)* 115.3 (2015), pp. 211–252. DOI: 10.1007/s11263-015-0816-y.

[57] Théo Ryffel et al. "Ariann: Low-interaction privacy-preserving deep learning via function secret sharing". In: *Proceedings on Privacy Enhancing Technologies* 2022.1 (2020), pp. 291–316.

[58] Shweta Shinde et al. "Preventing your faults from telling your secrets: Defenses against pigeonhole attacks". In: *arXiv preprint arXiv:1506.04832* (2015).

[59] Karen Simonyan and Andrew Zisserman. "Very deep convolutional networks for large-scale image recognition". In: *arXiv preprint arXiv:1409.1556* (2014).

[60] Alin Suciu and Tudor Carean. "Benchmarking the true random number generator of TPM chips". In: *arXiv preprint arXiv:1008.2223* (2010).

[61] Inc. Synopsys. *Synopsys tRoot Hardware Secure Modules*. URL: https://www.synopsys.com/designware-ip/security-ip/root-of-trust.html (visited on 10/03/2022).

[62] Florian Tramer and Dan Boneh. "Slalom: Fast, verifiable and private execution of neural networks in trusted hardware". In: *arXiv preprint arXiv:1806.03287* (2018).

[63] *Trusted Platform Module with SPI based on 32-bit ARM® SecurCore® SC300™ CPU*. https://www.st.com/resource/en/data_brief/st33tpm12spi.pdf. Nov. 2013.

[64] Jo Van Bulck, Frank Piessens, and Raoul Strackx. "SGX-Step: A practical attack framework for precise enclave execution control". In: *Proceedings of the 2nd Workshop on System Software for Trusted Execution*. 2017, pp. 1–6.

[65] Jo Van Bulck et al. "Foreshadow: Extracting the Keys to the Intel SGX Kingdom with Transient Out-of-Order Execution". In: *27th USENIX Security Symposium (USENIX Security 18)*. 2018, pp. 991–1008.

[66] Ashish Vaswani et al. "Attention is all you need". In: *Advances in neural information processing systems* 30 (2017).

[67] Sameer Wagh, Divya Gupta, and Nishanth Chandran. "SecureNN: 3-Party Secure Computation for Neural Network Training." In: *Proc. Priv. Enhancing Technol.* 2019.3 (2019), pp. 26–49.

[68] Sameer Wagh et al. "Falcon: Honest-majority maliciously secure framework for private deep learning". In: *arXiv preprint arXiv:2004.02229* (2020).

[69] Jinwen Wang et al. "Interface-based side channel attack against intel SGX". In: *arXiv preprint arXiv:1811.05378* (2018).

[70] Yongqin Wang et al. "Characterizing and Improving MPC-based Private Inference for Transformer-based Models". In: *NeurIPS 2021 Workshop Privacy in Machine Learning*. 2021.

[71] Thomas Wolf et al. "Transformers: State-of-the-Art Natural Language Processing". In: *Proceedings of the 2020 Conference on Empirical Methods in Natural Language Processing: System Demonstrations*. Online: Association for Computational Linguistics, Oct. 2020, pp. 38–45. URL: https://www.aclweb.org/anthology/2020.emnlp-demos.6.

[72] Yuanzhong Xu, Weidong Cui, and Marcus Peinado. "Controlled-channel attacks: Deterministic side channels for untrusted operating systems". In: *2015 IEEE Symposium on Security and Privacy*. IEEE. 2015, pp. 640–656.

[73] Andrew C Yao. "Protocols for secure computations". In: *23rd annual symposium on foundations of computer science (sfcs 1982)*. IEEE. 1982, pp. 160–164.

[74] Andrew Chi-Chih Yao. "How to generate and exchange secrets". In: *27th Annual Symposium on Foundations of Computer Science (sfcs 1986)*. IEEE. 1986, pp. 162–167.

[75] *ZeroMQ*. https://github.com/zeromq/libzmq.

[76] Wenting Zheng et al. "Helen: Maliciously secure coopetitive learning for linear models". In: *2019 IEEE Symposium on Security and Privacy (SP)*. IEEE. 2019, pp. 724–738.

[77] Xing Zhou et al. "PPMLAC: high performance chipset architecture for secure multi-party computation". In: *Proceedings of the 49th Annual International Symposium on Computer Architecture*. 2022, pp. 87–101.

A Basic MPC protocols

Correlated Randomness. A large number of random shares have to be obtained by the parties during the offline phase to reduce the communication cost during the offline phase. The 3-out-of-3 randomness is defined as each P_i holding a share of 0: $\alpha = [\![\alpha]\!]_1^L + [\![\alpha]\!]_2^L + [\![\alpha]\!]_3^L$ where $\alpha = 0$ and P_i holds $[\![\alpha]\!]_i^L$. They can be efficiently generated locally by a pseudo-random function (PRF). The security of the PRF function indicates that the output of a PRF is computationally indistinguishable (indistinguishable by a computationally bounded adversary) from the output of a truly random function. Given k_i as the key that P_i and P_{i+1} share through a key exchange protocol for each i and $\hat{F}$ as the PRF that is public to all parties, each P_i can generate shares $[\![\alpha]\!]_i^L$ as $[\![\alpha]\!]_i^L = \hat{F}_{k_i}(\text{ctr}) - \hat{F}_{k_i}(\text{ctr})$ with increments of ctr each time this process is invoked.

Input Phase. To construct $[\![x]\!]^L$ from the generated 3-out-of-3 randomness and $\bar{x}$ which is provided by P_i, P_i compute $[\![x]\!]_i^L = x + [\![\alpha]\!]_i^L$ and share it with P_{i-1}. P_{i-1} will send $[\![\alpha]\!]_{i-1}^L$ to P_{i+1} and P_{i+1} will send $[\![\alpha]\!]_{i+1}^L$ to P_i. In an honest majority malicious setting, additionally P_{i+1} should compute $[\![\alpha]\!]_{i+1}^L + [\![\alpha]\!]_{i-1}^L$ and send to P_i, then P_i confirm $[\![\alpha]\!]_{i+1}^L + [\![\alpha]\!]_{i-1}^L = -[\![\alpha]\!]_i^L$, therefore P_{i_1} behaves honestly; P_i should compute $[\![\alpha]\!]_{i+1}^L + [\![\alpha]\!]_i^L$ and send to P_{i-1}, then P_{i-1} confirm by $[\![\alpha]\!]_{i+1}^L + [\![\alpha]\!]_i^L = -[\![\alpha]\!]_{i-1}^L$, therefore P_{i+1} behaves honestly. Since P_i is allowed to send an arbitrary input $\bar{x}$, we do not need to check the share it sends.

Linear Operations. For RSS shared secrets, most linear operations can be performed locally. For shares $[\![x]\!]^L$, $[\![y]\!]^L$, and the public scalar c, we have the following:

- $[\![x]\!]^L + c = ([\![x]\!]_1^L + c, [\![x]\!]_2^L, [\![x]\!]_3^L)$

- $c \cdot [\![x]\!]^L = (c \cdot [\![x]\!]_1^L, c \cdot [\![x]\!]_2^L, c \cdot [\![x]\!]_3^L)$

- $[\![x]\!]^L + [\![y]\!]^L = ([\![x]\!]_1^L + [\![y]\!]_1^L, [\![x]\!]_2^L + [\![y]\!]_2^L, [\![x]\!]_3^L + [\![y]\!]_3^L)$

That can be done without any communication. However, multiplication between shared secrets cannot be done locally.

Reconstruction. $x \leftarrow \Pi_{\text{Reconst}}([\![x]\!]^L)$: To reconstruct the plaintext x from the shares $[\![x]\!]^L$, each party P_i will send $[\![x]\!]_i^L$ to P_{i+1} in the semi-honest setting. After completion, all parties have all 3 shares to reconstruct x. In a malicious setting, P_i will also send $[\![x]\!]_{i+1}^L$ to P_{i-1}. Then, under the honest majority assumption, at most one of the two copies of the share they receive is altered. A party can compare the values received from the other two and abort if an inconsistency occurs.

B Security Analysis

In this section, we analyze the security of our proposed techniques. We first define the ideal functionalities of the ML functions offered in our framework in Figure 5. We then state the following theorem:

Theorem 1. *Our protocol* Π_{STAMP} *securely realizes the ideal functionalities* $\mathcal{F}_{\text{STAMP}}$ *by Definition 1*

Proof. We construct a simulator $\mathcal{S}_{\text{STAMP}}$ such that a PPT environment $\mathcal{Z}$ cannot be able to distinguish between the real process and the ideal process. Note that the environment $\mathcal{E}$ selects inputs for the honest parties and obtains the corresponding outputs. The environment $\mathcal{E}$ can corrupt up to 1 out of 3 parties and takes control over its action, but not the LTEE component in the corrupted party. When $\mathcal{E}$ stops, it outputs a bit indicating whether $\mathcal{E}$ is interacting with real protocol or the simulated protocol. The simulator runs a copy of Π_{STAMP} protocol online, relays the messages between the parties and $\mathcal{E}$ such that $\mathcal{E}$ will see the same interface as when interacting with the real protocol. Figure 6 presents the specification of $\mathcal{S}_{\text{STAMP}}$.

We show that the view of $\mathcal{E}$ in the ideal process is indistinguishable from the view in the real process. The view contains the view of the corrupt party during protocol execution and the inputs/outputs of the honest parties. We argue that the view up to the point just before the output value is opened has the same distribution in the real and simulated case. Specifically, in the input phase, the values broadcast by honest players are uniformly random because of random masking. During each ML computation, the values that honest parties send out to other parties and receive from the other parties and the LTEE are all uniformly random and independent due to random masking generated by the trusted LTEE (e.g., Steps 1 and 4 in Protocol 4).

If the protocol proceeds to the last final output step, the only new data that $\mathcal{E}$ sees is the output value $\mathbf{y}$ of the ML computation plus some shares of honest parties. These are random shares consistent with $\mathbf{y}$ due to replicated secret sharing. In other words, given that $\mathbf{y}$ is identical, the environment's view of the output step has the same distribution in the real and simulated processes.

In the simulation, $\mathbf{y}$ is obviously the correct ML computation, as it is the output of the ideal functionality. We show that the same happens in the real protocol with overwhelming probability. In other words, the event that the real protocol terminates but the output is incorrect happens with negligible probability.

First, it is easy to see that the real protocol outputs the correct $\mathbf{y}$ in the semi-honest case due to the correctness of replicated secret sharing along with the consistency of masking and unmasking processes, which is guaranteed by the counters as described in §4.1. We show that if the adversary is malicious and deviates from the protocol, the real protocol will abort without returning an incorrect value with overwhelming probability. Incorrect outputs may arise from the corrupted party, who, during the execution of the protocol, successfully cheats with altered shares to the other parties without being detected. In our protocol, there are two different types of cases in which the adversary can cheat. The

first occurs during multiplication, where, as described in §3.2, each party would make a local calculation that changes the 2-out-of-3 RSS to 3-out-of-3 secret sharing. Each party would have one unique share of each secret, and if it alters it before resharing it cannot be caught by the semi-honest protocol. We use the malicious multiplication protocol introduced in [44, 14] to guarantee the verifiability of the shares. The protocol uses a pregenerated 2-out-of-3 RSS multiplication triple to verify another 2-out-of-3 RSS multiplication triple, in our case the multiplication inputs and results. The other type of cases is that, during any of the other protocols including all non-linear operations and the output phase, the malicious party can alter the share it sends during the protocol. We have addressed this with the blue steps in Protocol 4, Protocol 5, and Protocol 6. We take the example of step 2 of Protocol 4, and without loss of generality, we assume that P_1 is the malicious party. P_1 sends $\mathbf{x}'_1 + \varepsilon$ instead of the correct $\mathbf{x}'_1$ to P_2, P_2 can detect it by comparing it with the $\mathbf{x}'_1$ sent by P_3 because P_3 must be honest due to the honest majority assumption. □

C Privacy against Malicious Security

In this section, we discuss the security against malicious adversaries. Generally, compared to the semi-honest protocol, one same step occurs twice on different parties, and additionally for each transmission the receiver gets replicate copies from two parties. Checking the consistency of the two inputs can detect deviations from the honest protocol. In the following, we show Π_{ReLU} securely realizes $\mathcal{F}_{\text{ReLU}}$ with abort. Since additional transmission is done compared to semi-honest setting, we first analyze the secrecy when our protocol requires transmitting data transmission.

In step 1), P_{i+1}, P_{i-1} receives one pseudo-random vector and P_i receives two, these leak no information.

In step 2), P_i receives the same mask $\mathbf{x}'_{i-1}$ from the other two. It reviews no new information.

In step 4), P_i and P_{i+1} receive masked results. Again, they leak no information due to masking.

In step 5), P_{i-1} receives $[\![\mathbf{y}]\!]_{i-1}^L$ from P_i and P_{i+1} and $[\![\mathbf{y}]\!]_i^L$ from H_{i-1}, which are all masked. P_i and P_{i+1} receive both shares from their LTEE masked. All values are masked by one-time pads and, therefore, secure.

Now, we analyze the security against an active adversary with abort. Without loss of generality, assume that $i = 1$ in the protocol.

If P_1 is the adversary, they can:

- Send the altered results to P_2 in step 2). This will cause an abort in step 3) since P_2 will find an inconsistency by comparing copies from P_1 and P_3.

- Send altered results to H_1 in step 3), or send the altered results to P_2 and P_3 in step 5). These will cause abort in

Initialize. On input $(init, p^k)$ from all parties, the functionality activates and stores the modulus L.

Input. On input $(Input, n, Vid, \mathbf{X})$ from P_i where $\mathbf{x}$ is a vector of n entries, stores data $(Vid, \mathbf{x})$ with Vid being the fresh identifier.

ReLU. On command $(ReLU, n, Vid_1, Vid_2)$ where Vid_1 is in the storage while Vid_2 is not, get $\mathbf{x} = (x_1, \ldots, x_n)$ from Vid_1 and compute $y_i = \max(0, x_i)$ for $i = 1, \ldots, n$. Save $\mathbf{y}$ to Vid_2 as $(Vid_2, \mathbf{y})$.

MaxPool. On command $(MaxPool, n, Vid_1, Vid_2, Vid_3)$ where Vid_1 is in the storage while Vid_2 and Vid_3 are not, use stored $(Vid_1, \mathbf{x})$ to compute $k = \mathsf{argmax}(x_1, \ldots, x_n)$, $z = x_k$ and store (Vid_2, k), (Vid_3, z).

BatchNorm. On command $(BatchNorm, n, Vid_1, Vid_2, Vid_3, Vid_4)$ where Vid_1, Vid_2, Vid_3 are in the storage while Vid_4 is not, use stored $(Vid_1, \mathbf{x})$, (Vid_1, γ), (Vid_1, β) to compute $\mu = \frac{1}{n}\sum_{i=1}^{n} a_i$, $\sigma^2 = \frac{1}{n}\sum_{i=1}^{n}(a_i - \mu)^2$, $b_i = \gamma\frac{a_i-\mu}{\sigma^2} - \beta$, and store $(Vid_2, \mathbf{b})$.

Softmax. On command $(Softmax, n, Vid_1, Vid_2)$ where Vid_1 is in the storage while Vid_2 is not, use stored $(Vid_1, \mathbf{x})$ to compute $y_i = 1/(1 + \exp(-x_i))$ for $i = 1, \ldots, n$ and store $(Vid_2, \mathbf{y})$.

MatMalReLU. On command $(MatMalReLU, a, b, c, Vid_1, Vid_2, Vid_3)$ where Vid_1, Vid_2 are in the storage while Vid_3 is not, use stored $(Vid_1, \mathbf{A})$, $(Vid_2, \mathbf{B})$ (convert vectors to matrix using the input dimensions) to compute $\mathbf{C} = (\mathbf{A} \times \mathbf{B})$, $D_{i,j} = max(0, C_{i,j})$ and store $(Vid_3, \mathbf{D})$ (flat the matrix into a vector).

MatMalMaxPoolReLU. On command $(MatMalMaxPoolReLU, a, b, c, Vid_1, Vid_2, Vid_3, n, w, s, d)$ where n, w, s, d are matrix size, pool size, stride and padding length, Vid_1, Vid_2 are in the storage while Vid_3 is not. Use stored $(Vid_1, \mathbf{A})$, $(Vid_2, \mathbf{B})$ (convert vectors to matrix using the input dimensions) to compute $\mathbf{C} = \mathbf{A} \times \mathbf{B}$, $D_{i,j} = max\{0, C_{min(max(1,i*s-d+p),n), min(max(1,i*s-d+q),n)}\}$ for $p, q = 1, \ldots, w$, and store $(Vid_3, \mathbf{D})$ (flat the matrix into a vector).

MatMalBatchNormReLU. On command $(MatMalBatchNormReLU, a, b, c, Vid_1, Vid_2, Vid_3, \gamma, \beta)$ where w, s, d are pool size, stride and padding length, Vid_1, Vid_2 are in the storage while Vid_3 is not. Use stored $(Vid_1, \mathbf{A})$, $(Vid_2, \mathbf{B})$ (convert vectors to matrix using the input dimensions) to compute $\mathbf{C} = \mathbf{A} \times \mathbf{B}$, compute $\mu_i = \frac{1}{n}\sum_{j=1}^{n} C_{i,j}$, $\sigma_i^2 = \frac{1}{n}\sum_{j=1}^{n}(C_{i,j} - \mu_i)^2$, $D_{i,j} = max(0, \gamma_i\frac{C_{i,j}-\mu_i}{\sigma_i^2} - \beta_i)$, and store $(Vid_3, \mathbf{D})$) (flat the matrix into a vector).

Output. On command $(Output, n, Vid_1)$ from all parties, send the stored $(Vid_1, \mathbf{y})$ to the environment. If the environment inputs "OK" then $\mathbf{y}$ is output to all parties. If instead "abort" is received output "abort".

Figure 5: Ideal functionality of STAMP.

step 5) as P_2 /P_3 will find an inconsistency comparing the outputs of P_1 and P_3 /P_1 and P_2.

If P_2 is the adversary, they can:

- Send the altered results to H_2 in step 3), or send the altered results to P_1 and P_3 in step 5). These will cause abort at step 5) since P_1/P_3 will find inconsistency comparing outputs from P_2 and P_3/P_2 and P_1.

If P_3 is the adversary, they can:

- Send the altered results to P_1 in step 2). This will cause an abort in step 3) since P_1 will find an inconsistency by comparing copies from P_1 and P_3.

- Send altered results to H_3 in step 3), or send the altered results to P_1 and P_2 in step 5). These will cause abort in step 5) as P_1 /P_2 will find an inconsistency comparing the outputs of P_2 and P_3 /P_1 and P_3.

Additionally, if any of the parties has inconsistent shares of inputs in the beginning, they will be detected at step 2) or step 5) during the comparison of these steps. If in step 5) any

party alters the shares they created, it will be detected in the next operation, or during the malicious reconstruction mentioned in Appendix A. Therefore, we show that the protocol either outputs correct shares or aborts if any malicious behavior occurs. A similar argument goes to Π_{MaxPool}, $\Pi_{\text{BatchNorm}}$, $\Pi_{\text{LayerNorm}}$, and Π_{Softmax}.

The proof of $\Pi_{\text{MatMulReLU}}$ is intuitive by splitting it into two parts: Step 1) is just $\Pi_{\text{mal-arith-mult}}$ and is proven to be secure against malicious adversaries in [44]; Step 2) − 6) are then reduced to the same as Π_{ReLU} which we have just proven. The same argument goes for the proof of $\Pi_{\text{MatMulMaxPoolReLU}}$ and $\Pi_{\text{MatMulBatchNormReLU}}$.

D Efficiency

The cost analysis is shown in Table 7. The byte size of the finite field is chosen to be 4 and we count the exponent and the mantissa part in Protocol 6 as 4 and 8 bytes. AriaNN [57] results are from their articles. We see significant improvements in inter-party communication rounds compared to Falcon, and significant theoretical reduction in the amount of communication data compared to both Falcon and AriaNN.

Initialization. All parties start generating shares of zeros communicating through $\mathcal{S}_{\text{STAMP}}$.

Input. If P_i is not corrupted, then it executes the protocol honestly but $\mathcal{S}_{\text{STAMP}}$ only receives dummy inputs. If P_i is corrupted, the input phase is still executed honestly and $\mathcal{S}_{\text{STAMP}}$ obtains the input $\mathbf{x}_i$ by observing P_i's broadcast.

ReLU. $\mathcal{S}_{\text{STAMP}}$ executes the protocol honestly and signals "ReLU" command on the ideal functionality $\mathcal{F}_{\text{STAMP}}$ with parameters. **MaxPool** $\mathcal{S}_{\text{STAMP}}$ executes the protocol honestly and signals "MaxPool" command on the ideal functionality $\mathcal{F}_{\text{STAMP}}$ with parameters.

BatchNorm $\mathcal{S}_{\text{STAMP}}$ executes the protocol honestly and signals "BatchNorm" command on the ideal functionality $\mathcal{F}_{\text{STAMP}}$ with parameters.

Softmax $\mathcal{S}_{\text{STAMP}}$ executes the protocol honestly and signals "Softmax" command on the ideal functionality $\mathcal{F}_{\text{STAMP}}$ with parameters.

MatMulReLU $\mathcal{S}_{\text{STAMP}}$ executes the protocol honestly and signals "MatMulReLU" command on the ideal functionality $\mathcal{F}_{\text{STAMP}}$ with parameters.

MatMulMaxPoolReLU $\mathcal{S}_{\text{STAMP}}$ executes the protocol honestly and signals "MatMulMaxPoolReLU" command on the ideal functionality $\mathcal{F}_{\text{STAMP}}$ with parameters.

MatMulBatchNormReLU $\mathcal{S}_{\text{STAMP}}$ executes the protocol honestly and signals "MatMulMaxPoolReLU" command on the ideal functionality $\mathcal{F}_{\text{STAMP}}$ with parameters.

Output. $\mathcal{S}_{\text{STAMP}}$ signal "Output" command on the ideal functionality $\mathcal{F}_{\text{STAMP}}$ with parameters and receive the correct output $\mathbf{y}$ stored. $\mathcal{S}_{\text{STAMP}}$ has the shares of an dummy output $\mathbf{y}'$: $([\mathbf{y}']_1, [\mathbf{y}']_2, [\mathbf{y}']_3)$ calculated by parties using the dummy inputs. Select two honest parties P_i and P_{i+1} (which can be done due to honest majority assumption) and change the $[\mathbf{y}']_{i+1}$ share to $[\mathbf{y}']_{i+1} - \mathbf{y}' + \mathbf{y}$ to make the shares of $\mathbf{y}$. Then it simulates the opening of the $\mathbf{y}$ according to the protocol and send "OK" to $\mathcal{F}_{\text{STAMP}}$ if it terminates correctly.

Figure 6: Simulator for Π_{STAMP}.

Communication Type	Framework	ReLU	MaxPool	BatchNorm/ LayerNorm	Softmax
	Falcon+	10	$12(w^2-1)$	335	-
Network comm. rounds	AriaNN	2	3	9	-
	STAMP	2	2	2	2
	Falcon+	$16n$	$20m^2+4w^2$	$224n$	-
Network comm. data	AriaNN	$12n$	$((m-w)/s+1)^2(w^4+1)$	$72n$	-
	STAMP	$5n$	$\frac{2}{3}(2n+2w^2+5((m-w)/s+1)^2)$	$4n$	$\frac{20}{3}n$
LTEE comm.	STAMP	$\frac{25}{3}n$	$\frac{1}{3}(8m^2+8w^2+15((m-w)/s+1)^2)$	$\frac{16}{3}n$	$\frac{44}{3}n$

Table 7: Analytical cost analysis of the network communication rounds and amount (in Bytes) under the semi-honest setting, and the local bus communication with the LEE. Here, $n = m \times m$ is the input size, s is the stride, and the filter size is set to $w \times w$.

The actual speedup of a particular neural network depends on its structure including the ratio between linear and non-linear operations, the order of linear/non-linear operations/layers (which determines if protocols like Protocol 5 can be applied), the input dimensions, etc. The communication setting and the computational power also matter. We discuss the performance in §5.

E   Pure TEE Solution

We put the data obtained for the pure TEE solution here. Some data cannot be obtained due to the limit of the size of the SGX enclave.

Network	Network-A	Network-B	Network-C	LeNet
STAMP	0.0737	0.1172	0.6809	0.9693
Pure SGX	0.4616	0.4612	0.4612	0.5067
Network	AlexNet	Transformer	VGG16	ResNet18
STAMP	1.5644	0.5130	26.558	309.71
Pure SGX	5.0308	-	-	8.1562

Table 8: STAMP or SGX execution time. We use the semi-honesy LAN/GPU results of STAMP for a comparison.